Nucleation triggering methods in supercooled phase change materials (PCM), a review

Noé Beaupere, U. Soupremanien, Laurent Zalewski

Nucleation triggering methods in supercooled phase change materials (PCM), a review

N. Beaupere[1, 2, *], U. Soupremanien[1], L. Zalewski[2]

[1]Université Grenoble Alpes, CEA Grenoble, CEA/LITEN/DTNM/SA3D/LMCM, 38000 Grenoble, France
[2]Université d'Artois, EA 4515, Laboratoire de Génie Civil et géo-Environnement (LGCgE), F-62400 Béthune, France
noe.beaupere@cea.fr ; ulrich.soupremanien@cea.fr ; laurent.zalewski@univ-artois.fr
* Corresponding author: Tel: +33 4 38 78 14 69, Email: noe.beaupere@cea.fr (N. Beaupere)

Abstract
Supercooling is an undesired property of phase change materials due to the poorly predictable occurrence of crystallization during cooling. For such situations, the stored latent heat cannot be recovered which can be an issue for temperature-controlled applications. This review illustrates the techniques used for triggering crystallization in phase change materials having a supercooling property. The development of triggering devices should constitute a breakthrough for heat on demand applications, as heat can be released even when the temperature drops far below the liquidus temperature. Several techniques appear to be promising for nucleation triggering. They have been classified into two categories: passive (reduction of supercooling) or active (triggering of crystallization on demand) devices. They were accurately investigated for water freezing for: meteorological comprehension, food preservation or the pharmaceutical industry. In this paper, several nucleating agents (passive) have been explored, and most of them, added by 1 wt%, can decrease the supercooling degree by more than 90%. In addition, the heat would be immediately released on demand from a supercooled material by the use of seeding or electrofreezing (active methods). Solidification can also be externally triggered by the application of high pressure or ultrasonic waves (active). In addition to the analysis of the efficiency of the different techniques in terms of supercooling reduction, this review also discusses the solidification process at a microscopic scale.

Keywords: Thermal energy storage; Phase Change Materials; Supercooling; Solidification;

Nomenclature

DSP	DiSodium Phosphate dodecahydrate
ΔG	Free energy variation (J)
Δg	Free energy variation per unit volume ($J.m^{-3}$)
L	Latent heat of fusion ($J.g^{-1}$)
N/A	Not Available
P	Relative pressure (Pa)
PCM	Phase Change Material
r	Radius of the nuclei (m)
TBAB	Tetra-n-butylammonium bromide
T	Temperature (K)
ΔT	Supercooling degree (K)
US	Ultrasound
Δv	Specific volume change ($m^3.kg^{-1}$)

Greek letters

γ	Surface tension ($J.m^{-2}$)
θ	Contact (wetting) angle between the solid and liquid surface (rad)

Subscript

x_F	Freezing
x_m	Melting
x_{SL}	Solid-Liquid
x_S	Related to surface
x_V	Related to volume

Superscript

x^*	Critical value

1. Introduction

Global warming is one of the major issue of the century, expected to be partly solved by the massive use of renewable energies. However, most of these energies are available randomly, which makes their integration in the electrical grid complicated. In addition to this, the energy consumption is far to be steady state as peak loads may occur daily, weekly or during the alternating seasons. Therefore, managing the temporal mismatch between our energy consumption and renewable energy availability is one of the major issues faced by our civilizations.

Thermal energy storage (TES) may help to solve this mismatch to a certain extent. Indeed, thermal energy could be stored when the source is available, resulting in an increase in energy capacity when it is needed. In addition, the integration of a thermal storage material that presents a phase change from solid to liquid (and vice versa) within the temperature range of the application will permit additional energy to be stored and released due to the melting/freezing processes. These materials, known as Phase Change Materials, are devoted to different applications depending on their melting temperatures (or on their classes). Some classes have been presented in Figure 1-Figure 2.

The biggest field of application is building, where Phase Change Materials with a melting temperature ranging between 270 K and 300 K (cooling) and from 320 K to 330 K (hot water production) are often used [1–6]. Another field of application is the automotive industry, where PCMs are used within a 270-1070 K temperature range [7] for emission reduction or electrical battery thermal management.

They are also promising for thermal protection of electronics [8–10].

Applications are paying particular attention to some properties of these materials:

- Storage capacity: adapted melting temperature, high density, high latent and specific heats;
- Delivery capability: high thermal conductivity, no supercooling;
- Cycling resistance: no decomposition, no segregation;
- Safety: chemical compatibility with the surrounding materials, non-flammable, non-explosive, non-toxic, low volume variation;
- Economic: available, low-cost, recyclable.

Phase Change Materials usually have a passive behavior as they melt above the liquidus temperature and solidify when the temperature drops below this temperature. However, as the crystallization and the melting point are usually similar, the heat cannot be released at any desired temperature. This could be an issue as the energy is not necessarily useful as soon as the temperature decreases but may be needed later, for heating up a device or for seasonal thermal storage, for example.

A solution to release energy at other temperatures compared to the liquidus temperature may rely on the understanding of the supercooling behavior. Supercooling is a metastable property, where the material remains liquid several degrees below its liquidus temperature. The latent energy, which could be particularly high for some of the materials exhibiting supercooling, will be kept as long as the material is liquid, and could be released on demand by solidifying the material. Although supercooling can be particularly significant for some materials, up to a hundred of degrees [11] for salt hydrates or sugar alcohols, it is generally avoided by the addition of nucleating agents for a better nucleation ability [12].

Some devices have been developed to store thermal energy under a supercooled state in buildings [13] or in thermodynamic solar panels [14] where a solid crystal of sodium acetate trihydrate was released in a supercooled liquid using a nucleation technique known as seeding.

This review will detail the different techniques that have been used to trigger nucleation of supercooled materials, first by introducing an analysis made with water and then by focusing on Phase Change Materials.

2. Supercooled Phase Change Materials

2.1. PCM classification

The first classification of Phase Change Materials, given in Figure 1, has been developed by Abhat [15] and later completed by Zalba et al. [16]. Each kind of materials has different properties and this review focuses on materials having a solid-liquid transition that can present a supercooled state such as sugar alcohols, hydrated salts, and fatty acids.

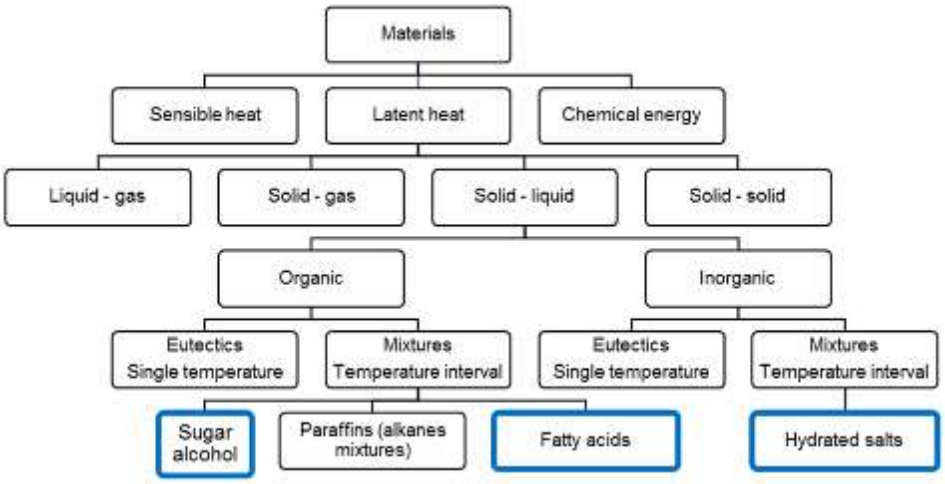

Figure 1 Classification of heat storage materials, a particular focus will be made in this review on the framed bold materials. Reprinted from [16], Copyright 2003, with permission from Elsevier (Single column image)

In Figure 2, the different classes of Phase Change Materials within a wide range of temperatures, from 170 K to 1070 K, with an almost linear variation of the volumetric latent heat of fusion reported.

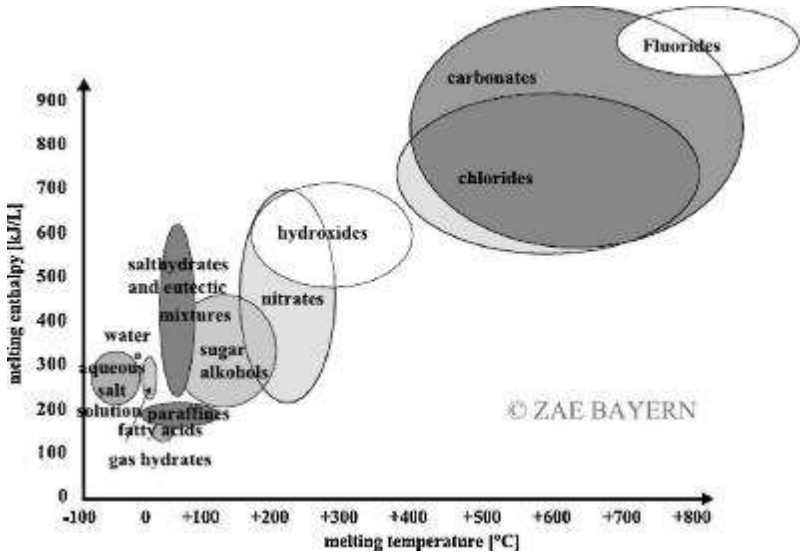

Figure 2 Classes of materials that can be used as PCM. Reprinted from [17], Copyright 2011, with permission from Elsevier. (Single column image)

A typical comparison of the properties of these materials is presented in Figure 3. Values were taken from the literature for salt hydrates (65 different materials), paraffins (40 materials, C_nH_{2n+2} with n = 10-100), sugar alcohols (29 different materials), fatty acids (11 different materials). The values plotted are averaged values for these materials, the highest value is set at 1 and lowest at 0, the values were then plotted as Eq 1.

$$value\ (\%) = 100 \times (value - lowest\ value)/(highest\ value - lowest\ value) \qquad \text{Eq 1}$$

The range of values from 0 to 100% is given as follow (as the mean value for the different classes):

- melting point from 310 to 387 K;
- supercooling degree from 0 to 72 K;
- density (solid) from 0.8 to 1.7;
- thermal conductivity (solid) from 0.13 to 1.07 $W.m^{-1}.K^{-1}$;
- latent heat of fusion (volume) from 180 to 370 $J.m^{-3}$;
- specific heat of the PCM (in the solid phase) from 1.32 to 2.09 $J.g^{-1}.K^{-1}$.

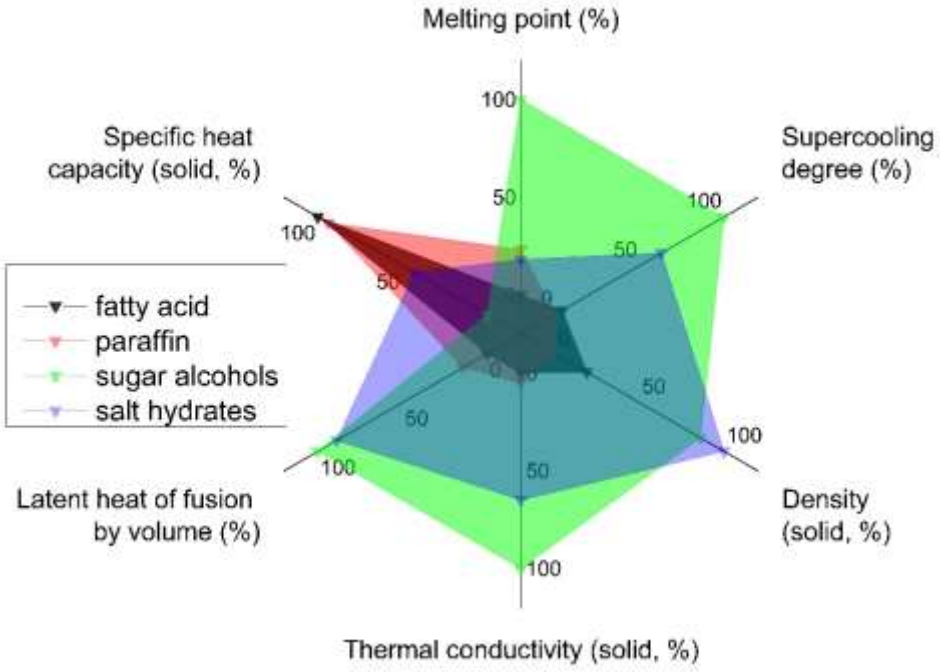

Figure 3 Properties of the relevant Phase Change Materials. (Two columns image)

From Figure 3, two groups of materials appear. First (salt hydrates + sugar alcohols), with good storage ability. They have a high latent heat by volume or by mass (because of a high density) and a high thermal conductivity, resulting in a fast release of heat. They are also subjected to a deep supercooling, as heat would be released through a large range of temperatures. Finally, a minimal heat loss through the supercooling stage will be allowed by a low specific heat. Thanks to different melting temperatures, these materials can be selected for thermal energy storage in a supercooled state and would be adapted to different kind of applications. The second group is composed of (fatty acids+paraffins) whose properties are, on the contrary, not adapted for long-term energy storage.

For this study, only materials experiencing supercooling around room temperature will be studied.

2.2. Typical properties of supercooled PCMs

The supercooling degree represents the range of temperature where the material remains liquid below its melting point. It is defined by the difference between the onset temperature of the melting and the freezing process, as given in Eq 2.

$$\Delta T = T_m - T_F \quad \text{Eq 2}$$

This supercooling degree appears to be influenced by different factors. For instance, it can be increased by dividing the bulk volume to microscopic size using encapsulation or an emulsion technique [18], because each capsule will contain a non-sufficient number of impurities. Adachi et al. [11] present an increase of 30 K in supercooling, ranging from 48 K to 78 K when the sample volume was decreased from 16 cm^3 to 0.025 cm^3. It would also be influenced by the crystal structure of any surface, such as the container's ones [19] and their roughness [20].

Another factor is the cooling rate. If the temperature is decreased fast enough, the viscosity will increase, resulting in the impossibility for the particle to aggregate to form a crystal. The material will become amorphous without releasing its energy before being reheated, a process known as cold crystallization. A study performed on D-Mannitol ($C_6H_{14}O_6$) showed that a cooling rate above 10 $K.min^{-1}$ would result in a cold crystallization [21]. Mollova et al. [22] presented the effect of the cooling rate on Polyamide 11, where the supercooling degree moved from 15 K to 90 K when the cooling rate increased from 0.01 $K.s^{-1}$ to 300 $K.s^{-1}$ (Figure 4).

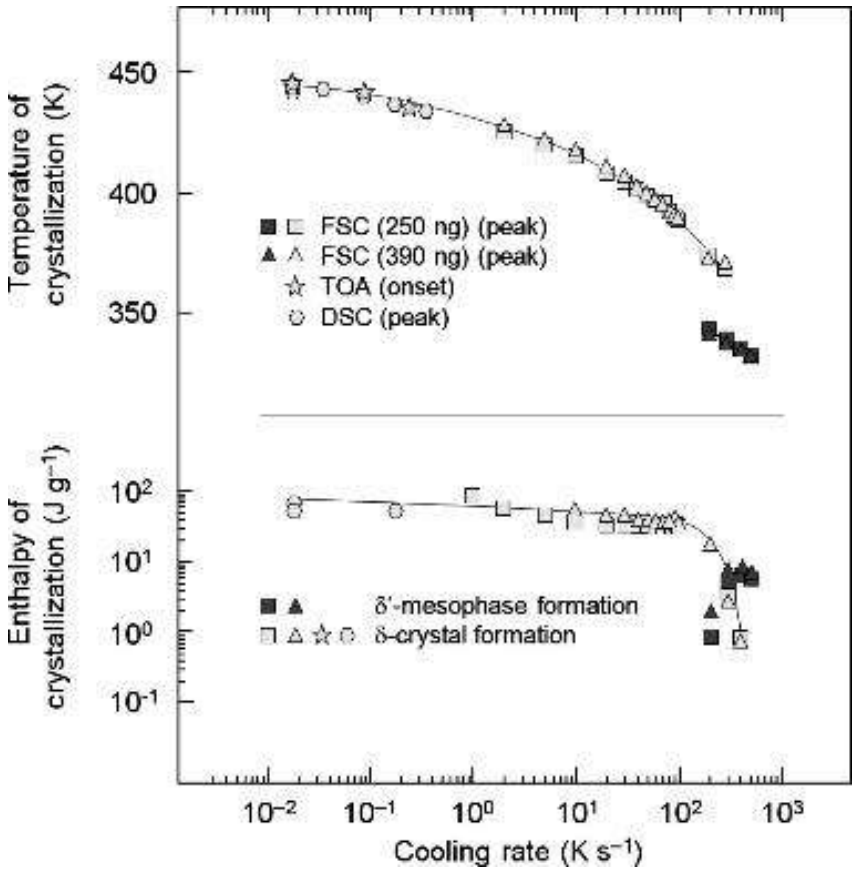

Figure 4 Temperature (top) and enthalpy of crystallization/ordering (bottom) of PA 11 as a function of the cooling rate (melting point: 459 K) Reprinted with permission from [22]. Copyright 2013, American Chemical Society. (Single column image)

Tables 1 to Tables 4 are given for the different classes of PCM to provide an overview of the thermal properties and supercooling degree. Only fatty acids, sugar alcohols, and salt hydrates are selected

because many of these materials have a melting point close to a common building or automotive applications, with latent heat higher than 150 J/g and many of them are subject to supercooling.

Fatty acids ($CH_3(CH_2)_nCOOH$) often have a lower latent heat of fusion than paraffins [7] and low supercooling (usually less than 5 K [23]). They also have a low heat conductivity, reducing their ability to release the heat when it is needed. Some of their properties are presented in Table 1. Their supercooling degree is usually not high enough to require a triggering technique for heat release in applications.

Table 1 List of fatty acids with supercooling values

Name (Formula)	Melting point (K)	Latent heat of fusion ($J.g^{-1}$)	Supercooling degree (K)	Cooling rate ($K.min^{-1}$)	Sample mass (mg)	Ref
Caprylic acid ($C_8H_{16}O_2$)	288	158	6.2	10	5	[24]
Capric acid ($C_{10}H_{20}O_2$)	305	153	2.6	5	5-10	[16] [23]
Lauric acid ($C_{12}H_{24}O_2$)	317	155	2.7	1	N/A	[25]
Myristic acid ($C_{14}H_{28}O_2$)	328	194	3.4	1	N/A	[25]
Palmitic acid ($C_{16}H_{32}O_2$)	336	206	3.9	1	N/A	[25]
Stearic acid ($C_{18}H_{36}O_2$)	342	215	0	1	N/A	[25]

Sugar alcohols ($C_nH_{2n+2}O_n$), can present higher melting points, larger latent heats of fusion, particularly by volume due to a high density, and important supercooling, up to 150 K, where the material can become glassy because of its high viscosity. Then, the atoms would not be allowed to move in order to form nuclei big enough to induce solidification. Therefore, the need for solidification triggering appears to be necessary. Table 2 gives the supercooling values of some of them.

Table 2 List of sugar alcohols with supercooling values

Name (Formula)	Melting point (K)	Latent heat of fusion ($J.g^{-1}$)	Supercooling degree (K)	Cooling rate ($K.min^{-1}$)	Sample mass (mg)	Ref
d-Threitol ($C_4H_{10}O_4$)	359	219	64	2-20	8	[26]
Xylitol ($C_5H_{12}O_5$)	365	249	70	0.5	2000	[27]
Sorbitol ($C_6H_{14}O_6$)	366	174	63	2	15	[28]
Adonitol ($C_5H_{12}O_5$)	375	220	26	5	5-10	[29]
d-Arabitol ($C_5H_{12}O_5$)	376	255	28	5	5-10	[29]
Resorcinol ($C_6H_6O_2$)	384	180	140	2		[30], [31]
Erythritol ($C_4H_{10}O_4$)	391	336	100	0.5	0.03-20	[11]
Mannitol ($C_6H_{14}O_6$)	439	316	62	10	N/A	[32,33]
Galactitol ($C_6H_{14}O_6$)	460	357	57	10	N/A	[33]

Salt hydrates are materials that can exhibit high supercooling degrees, up to 100 K, with a melting point close to room temperature, between 270 K and 400 K. These materials are usually cheap and easily available. However, they have some drawbacks such as a segregation effect also, resulting in an important decrease of latent heat after days [34]. Some of them are presented in Table 3.

Table 3 List of salt hydrates with supercooling value

Name (Formula)	Melting point (K)	Latent heat of fusion ($J.g^{-1}$)	Supercooling degree (K)	Cooling rate ($K.min^{-1}$)	Sample mass (mg)	Ref
Lithium chlorate trihydrate ($LiClO_3.3H_2O$)	281	253	6	N/A	N/A	[16], [35]
Potassium fluoride tetrahydrate ($KF.4H_2O$)	291.5	231	33	0.2	12	[36], [37]
Manganese(II) nitrate hexahydrate ($Mn(NO_3)_2.6H_2O$)	298	128	20	5	10	[38]
Calcium chloride hexahydrate ($CaCl_2.6H_2O$)	302	191	30	0.2	12	[37]
Lithium nitrate trihydrate ($LiNO_3.3H_2O$)	302	231	40	10	10-15	[36], [39]
Sodium sulfate decahydrate ($Na_2SO_4.10H_2O$)	305	186	20	N/A	80000	[36], [12]
Calcium bromide hexahydrate ($CaBr_2.6H_2O$)	307	115	60	N/A	N/A	[36]
Sodium hydrogen phosphate dodecahydrate ($Na_2HPO_4.12H_2O$)	308	280	20	N/A	80000	[36], [12]
Calcium nitrate tetrahydrate ($Ca(NO_3)_2.4H_2O$)	320	153	65	N/A	N/A	[40], [41]
Sodium thiosulfate pentahydrate ($Na_2S_2O_3.5H_2O$)	321	201	65	N/A	N/A	[36]
Sodium acetate trihydrate ($CH_3COONa.3H_2O$)	331	226	90	0.2	12	[36], [37]
Trisodium phosphate dodecahydrate ($Na_3PO_4.12H_2O$)	338	190	30	N/A	50000	[40], [42]
Tetrasodium diphosphate decahydrate ($Na_4P_2O_7.10H_2O$)	343	184	70	N/A	N/A	[16], [36]
Aluminum sulfate octadecahydrate ($Al_2(SO_4)_3 \cdot 18H_2O$)	361	219	27	N/A	85	[43], [44]
Magnesium nitrate hexahydrate ($Mg(NO_3)_2.6H_2O$)	363	163	70	N/A	N/A	[36]
Lithium perchlorate trihydrate ($LiClO_4.3H_2O$)	369	311	14	2	33.8	[28]
Lithium hydroxide monohydrate ($LiOH.H_2O$)	381	350	8.4	2	30	[28]
Magnesium chloride hexahydrate ($MgCl_2.6H_2O$)	390	169	80	N/A	N/A	[36]
Zinc ammonium sulfate hexahydrate ($(NH_4)_2Zn(SO_4)_2.6H_2O$)	396	222	85	2	41.6	[28]

According to Table 1 to Table 3, a large number of materials with high latent heat and a melting point close to ambient temperature also present a large supercooling.

For thermal energy storage, the material needs to be supercooled at room temperature, assumed to be between 288 K and 298 K, as the latent heat would be stored for a long time with no need for insulation. Some of the materials having this property are given in Table 4.Triggering methods for

these materials will be presented, and studies on water, where the mechanism tends to be understood, will be added.

Table 4 Materials in a metastable (liquid) state around 293 K

Type	Name (Formula)	Melting point (K)	Latent heat of fusion ($J.g^{-1}$)	Supercooling degree (K)	Ref
Fatty acid	Caprylic acid ($C_8H_{16}O_2$)	288	158	6.2	[24]
Salt hydrates	Potassium fluoride tetrahydrate ($KF.4H_2O$)	291,5	231	33	[36], [37]
	Manganese(II) nitrate hexahydrate ($Mn(NO_3)_2.6H_2O$)	298	128	20	[38]
	Calcium chloride hexahydrate ($CaCl_2.6H_2O$)	302	191	30	[37]
	Lithium nitrate trihydrate ($LiNO_3.3H_2O$)	302	231	40	[36], [39]
	Sodium sulfate decahydrate ($Na_2SO_4.10H_2O$)	305	186	20	[36], [12]
	Calcium bromide hexahydrate ($CaBr_2.6H_2O$)	307	115	60	[36]
	Sodium hydrogen phosphate dodecahydrate ($Na_2HPO_4.12H_2O$)	308	280	20	[36], [12]
	Calcium nitrate tetrahydrate ($Ca(NO_3)_2.4H_2O$)	320	153	65	[16], [41]
	Sodium thiosulfate pentahydrate ($Na_2S_2O_3.5H_2O$)	321	201	65	[36]
	Sodium acetate trihydrate ($CH_3COONa.3H_2O$)	331	226	90	[36], [37]
	Tetrasodium diphosphate decahydrate ($Na_4P_2O_7.10H_2O$)	343	184	70	[16], [36]
	Magnesium nitrate hexahydrate ($Mg(NO_3)_2.6H_2O$)	363	163	70	[36]
Sugar alcohols	d-Threitol ($C_4H_{10}O_4$)	359	219	64	[26]
	Xylitol ($C_5H_{12}O_5$)	365	249	70	[27]
	Resorcinol ($C_6H_6O_2$)	384	180	140	[30], [31]
	Erythritol ($C_4H_{10}O_4$)	391	336	100	[11]

3. Theory of heterogeneous nucleation

The free energy change of a growing crystal can be expressed with Eq 3 [45].

$$\Delta G = \Delta G_s + \Delta G_v = 4\pi r^2 \gamma_{SL} + 4\pi r^3 \Delta g/3 \quad \text{Eq 3}$$

where Δg is the free energy change per volume unit ($J.m^{-3}$), calculated using Eq 4.

$$\Delta g = L\Delta T/T_m \quad \text{Eq 4}$$

This equation expresses two competitive effects: a surface effect, which tends to reduce the particle size to decrease the energy and increase stability, and a volume effect which tends to increase its size to increase stability. In Figure 5, total (ΔG), surface (ΔG_s) and volume (ΔG_v) free energy variations are plotted.

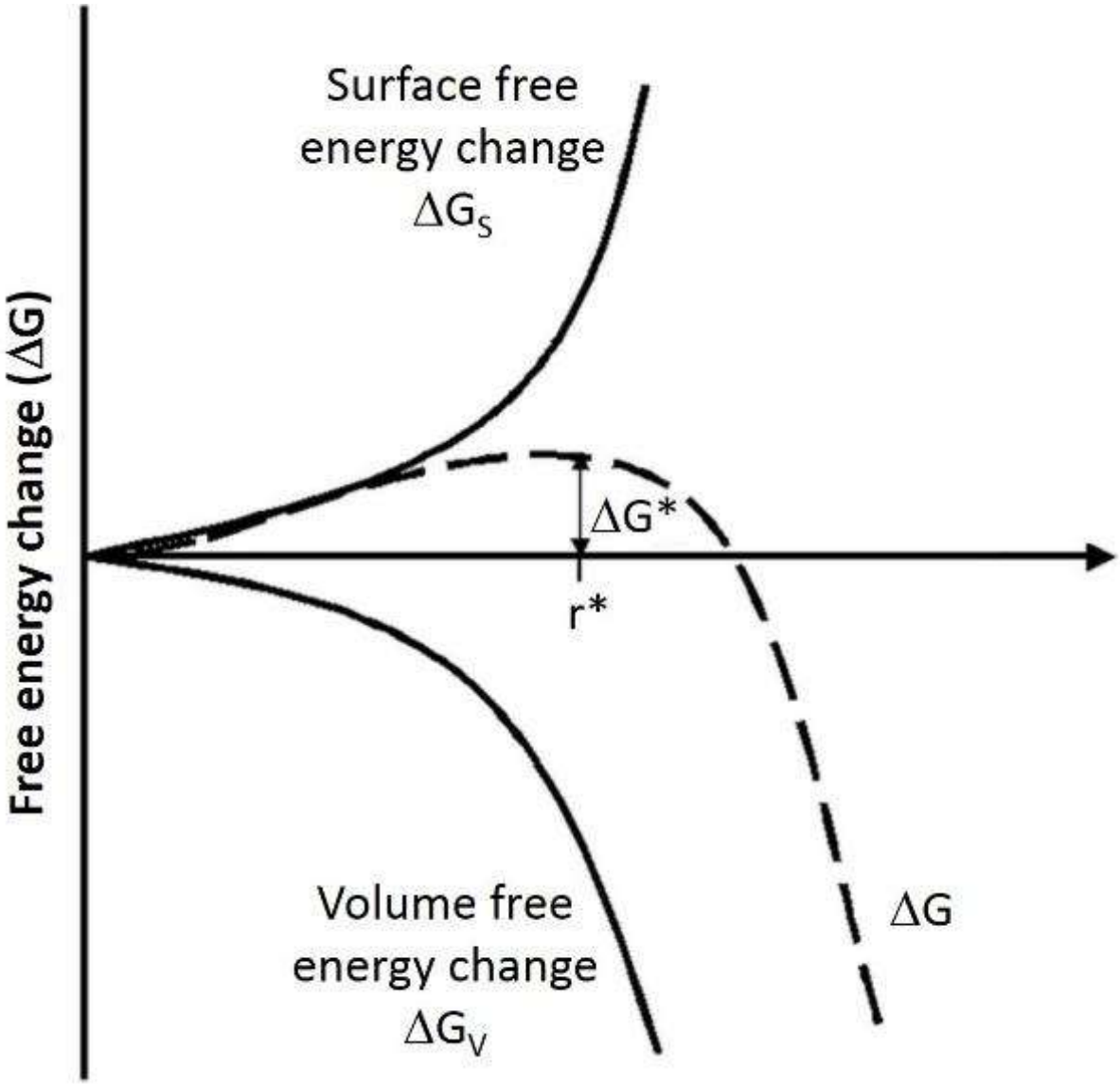

Figure 5 Energy competition in a nucleation event. Adapted from Ref. [46] with permission from the Royal Society of Chemistry. (Single column image)

The nuclei critical radius which is the minimum value needed to create a stable crystal, corresponds to the maximal value of Eq 3, setting $d\Delta G/dr = 0$ when $r = r^*$.

$$d\Delta G/dr = 8\pi\gamma_{SL} + 4\pi(r^*)^2\Delta g = 0 \qquad \text{Eq 5}$$

The critical radius can then be calculated as (Eq 6).

$$r^* = -2\gamma_{SL}/\Delta g = 2\gamma_{SL}T_m/L\Delta T \qquad \text{Eq 6}$$

The variation of free energy needed for the formation of a crystal is calculated (Eq 7) by replacing r^* (Eq 6) in Eq 3 [47].

$$\Delta G^*_{homogeneous} = 16\pi{\gamma_{SL}}^3/3(\Delta g)^2 = 4\pi\gamma(r^*)^2/3 = 16\pi{\gamma_{SL}}^3T_m^2/3(L\Delta T)^2 \qquad \text{Eq 7}$$

Therefore, the nucleation ability of a material is governed by both material parameters (T_m, L) and experimental parameters ($\Delta T, \gamma$). Supercooling reduction, to trigger nucleation, can be accomplished by modifying the experimental parameter, for example by putting the liquid material in contact with an existing surface, acting as a support for nucleation. This triggering is known as heterogeneous

nucleation. The surface can be made of the same material (known as seeding) or be made of a different material (acting as a nucleating agent). The critical free energy difference is then equal to (Eq 8).

$$\Delta G^*_{heterogeneous} = \Delta G^*_{homogeneous} \times (2 + cos\,\theta)(1 - cos\,\theta)^2/4 \quad \text{Eq 8}$$

The energy change required is decreased by the presence of this surface, as the wettability of the liquid is increased (decrease of the contact angle), as plotted in Figure 6.

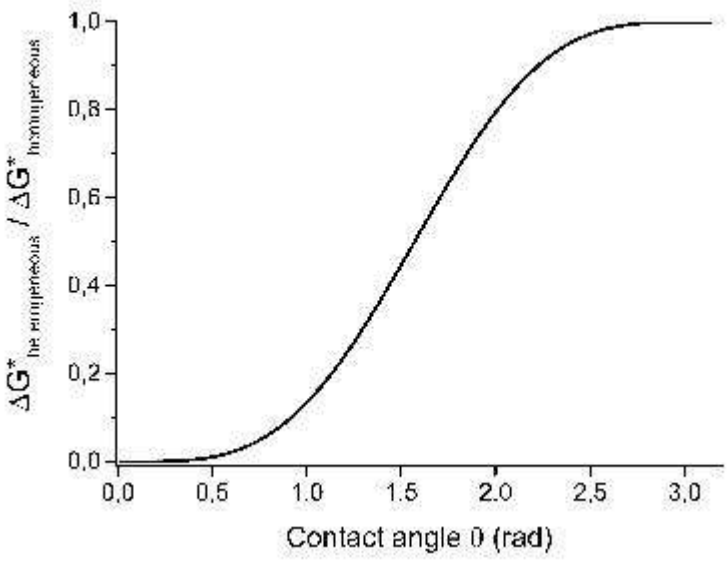

Figure 6 Variation of the critical energy required for nucleation, depending on the contact angle. (Single column image)

Another way to trigger nucleation is to increase the supercooling degree, by decreasing the temperature or increasing the melting point (by pressure variation).

4. Triggering methods

Several methods have been studied to initiate the solidification process from a supercooled liquid as the solidification process and heat release are controlled by the nucleation triggering. These methods were shown to be effective for water crystallization [48] and were also tested using some of the materials among the one presented above with different devices. The goal was to find the best combination of material and triggering techniques for each application.

4.1. By contacting a surface with the supercooling liquid

Placing a supercooled material in contact with a surface will facilitate the heterogeneous nucleation process where the nucleation starts from a substrate. This substrate can be:

- A solid particle from the same material type as the surrounding liquid;
- A solid particle of a different material;
- Any external wall or edges in contact with the liquid.

4.1.1.Seeding

Seeding is the easiest way to trigger nucleation of supercooled materials, by providing a stable solid crystal from the same material. The surrounding liquid will rapidly grow around this seed, because this structure modification will increase the stability, and heat will be released. Experimental work with seeding has been performed by several authors, because of its reproducibility and its effective heat release ability [49–51].

The major issue for nucleation triggering by seeding is to keep solid seed crystals while melting the phase change material. This can be achieved by applying very high pressure locally to increase the melting point of only a few particles. The relation between pressure and nucleation temperature is expressed by the Clausius-Clapeyron's equation, as in Eq 9.

$$\Delta T_m|_p/\Delta P = T_m|_{p=0}\,\Delta v/L \qquad \text{Eq 9}$$

According to Eq 9, a sharp increase in pressure will result in the increase of the melting point of the material. However, this equation is not representative of salt hydrate behavior and can be replaced by the Simon-Glatzel's equation as in Eq 10 [52].

$$\Delta T_m|_p/\Delta P = \left(T_m|_{p=0}\right)^c/acT_m^{c-1} \qquad \text{Eq 10}$$

where a (Pa) and c are fitting coefficients, determined by Barett et al. for several salt hydrates[53,54]. The relation was first experimentally investigated by Barrett et al. [55] as a way to trigger nucleation. The experimental procedure was to save a crystal from melting by clamping it between two pieces of different materials with known hardness. It was shown that an increase in pressure could increase the melting temperature. Another work, performed by Günther et al. [56], presents melting curves of salt hydrates well fitted by this polynomial equation. Besides, it is shown that the freezing curve is following the same slope, both with calculation and experimental investigation. These studies are summarized in Figure 7. It can be seen that most of the materials are subjected to an increase in melting point when a high pressure is applied.

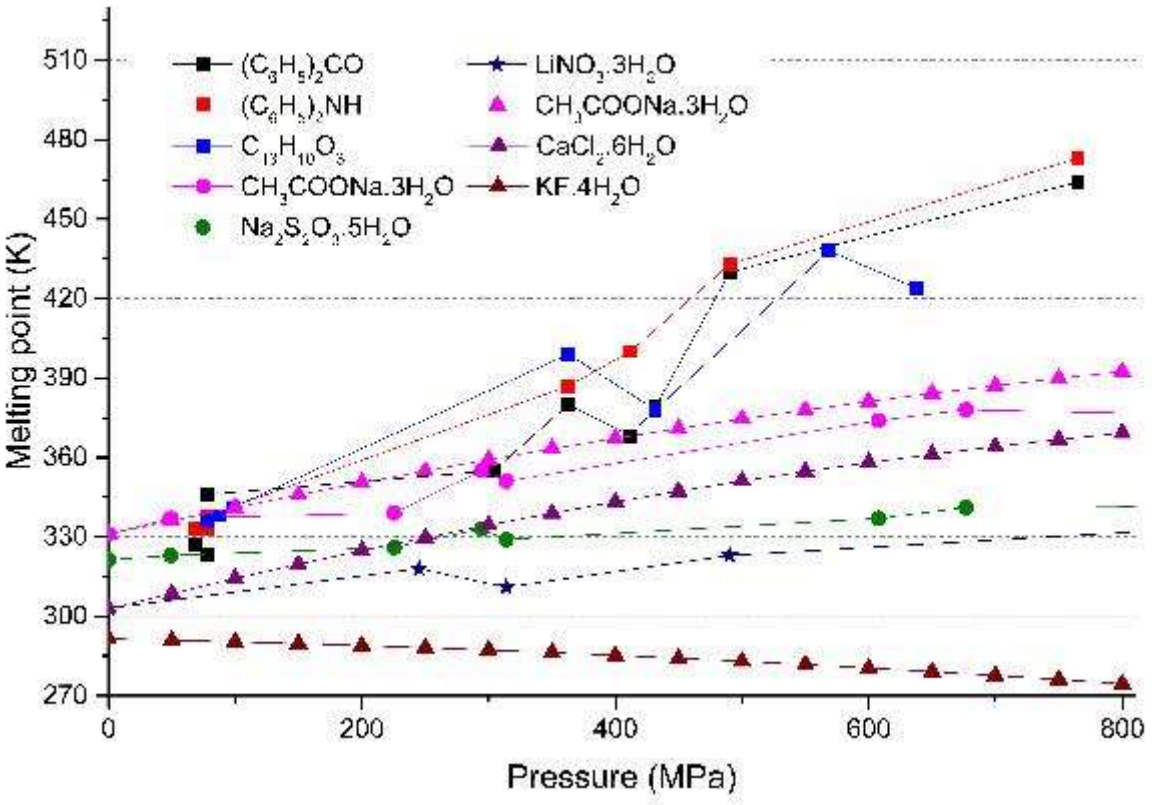

Figure 7 Melting temperatures of solid crystals at different pressures. Triangle-shaped curves, adapted from Günther et al. [56] (use of an autoclave for pressure application), square, round and star-shaped curves, adapted from Barrett et al. [53–55] (use of a material clamping for pressure application). (Single column image)

This method is used in a great number of applications, such as the commercial reusable heat pack. This device presents a small piece of metal, which is designed with some contact junctions, where solid crystals can easily be trapped under high pressure related to the hardness of the material, as presented in Figure 8a. Then, the seed crystal can be released in the supercooled liquid by flexing a piece of metal. A work by Sandnes [57] also proved that seeding was due to the release of pressure of a trapped solid crystal (analysis based on the study of different triggering devices, Figure 8b).

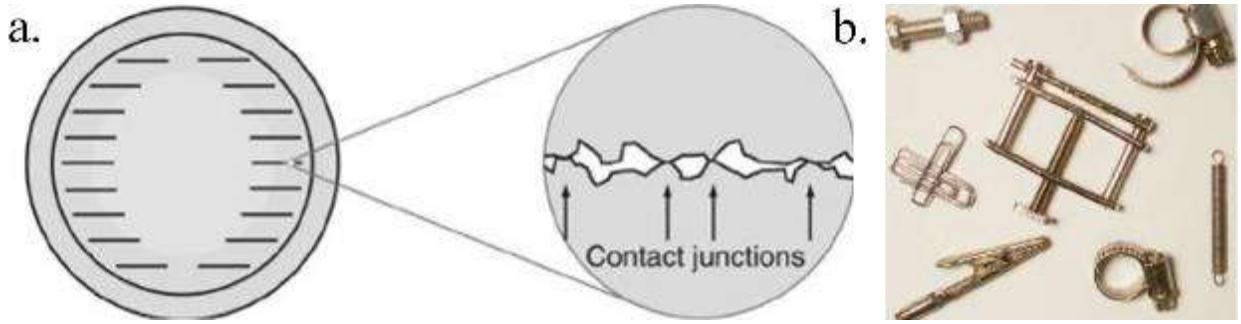

Figure 8 The triggering devices tested by Sandnes a) Piece of metal in the reusable heat pack. b) Alternative triggering devices. Reproduced from [57] with the permission of the American Association of Physics Teachers. (Single column image)

Whereas some materials can reach a large degree of supercooling, they will completely solidify as soon as a seed crystal is introduced inside the supercooled material, resulting in a large amount of heat released and a sharp increase in temperature, as presented in Figure 9.

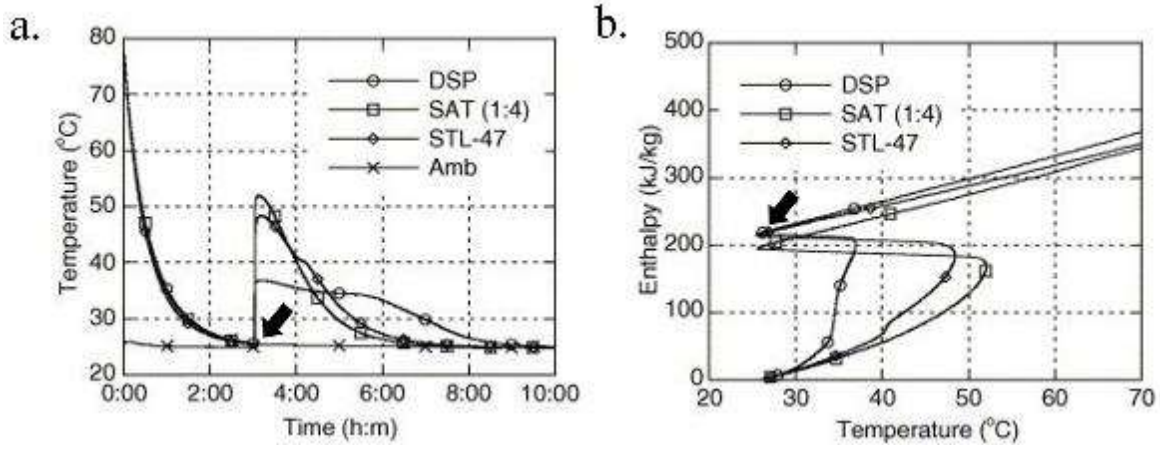

Figure 9. Measured enthalpies (a) and temperatures (b) as the PCM supercool. Seeding, indicated by arrows, after 3 h results in a sharp temperature increase. Adapted from [49], Copyright 2005, with permission from Elsevier. (Two columns image).

4.1.2.Nucleating agents

Another method for seeding is to use particles from another material. This material must have a higher melting point to remain solid when the PCM is melted. During cooling, the material will serve as a substrate for heterogeneous nucleation. Nucleating agents have regained interest for years with studies performed on many supercooled PCMs, as shown in Figure 10.

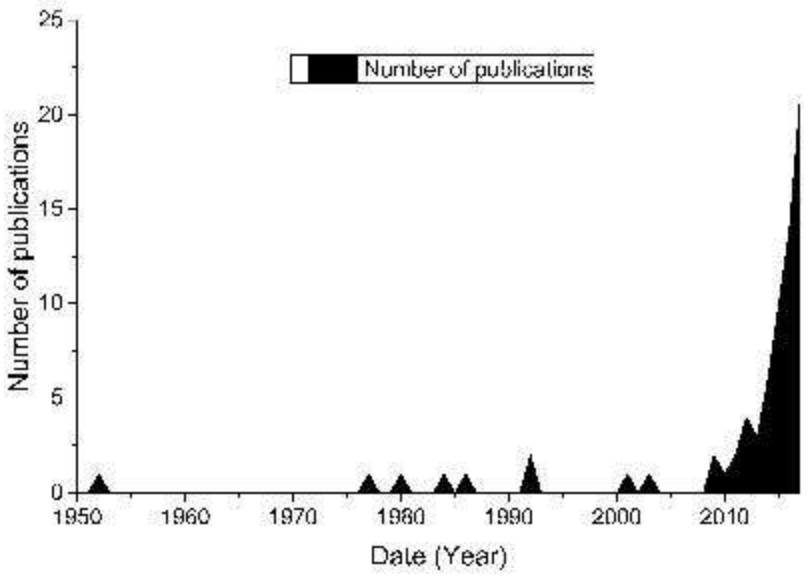

Figure 10. Publications per year for the use of nucleating agent as a nucleation triggering techniques of supercooled PCMs (from the Scopus search with the following keywords: "nucleating agent" AND (pcm OR "phase change material") AND (nucleat* OR solidif* OR crystal*) AND (supercooling OR undercooling OR subcooling OR sub-cooling). (Single column image)

The first publication from Figure 10, by Telkes [58], gave the rule that nucleating agents must have less than 15% variation in the unit cell dimension, in comparison to the PCM they nucleate, so that it can grow from the existing structure. This was supported by the work of Turnbull [59]. In Table 5, the materials to nucleate (on the left) and the nucleating agents covering a large number of materials (±15% of the dimension of a cubic unit cell) have been reported.

This rule of 15% was followed by many researchers, like Lane [12] who published a very detailed study of nucleating agents for different materials, testing both isostructural (within the 15% rule) and non-isostructural nucleating agents.

Table 5 Dimensions of the unit cell of cubic crystal structures with nucleated materials (left) and nucleating agents (right) [58]

Material	Dimensions of the unit cell (Å)	Nucleating agents (Dimensions of the unit cell, in Å)
LiCl	5.14	-15% (4.43) MnS (5.21) +15% (5.99)
KF	5.33	
LiBr	5.49	-15% (5.07) PbS (5.97) +15% (6.87)
NaCl	5.63	
RbF	5.63	-15% (5.21) PbSe (6.14)
NaBr	5.94	
LiI	6.00	-15% (5.39) PbTe
CsF	6.00	
KCl	6.28	
NaI	6.46	
KCN	6.55	

RbCl	6.57		(6.34)
KBr	6.57		
KI	7.05	+15% (7.06)	+15% (7.29)
NH_4I	7.24		
RbI	7.33		

A list of the different Phase Change Materials with high supercooling (at least 10 K supercooling), such as sugar alcohols and salt hydrates, and their nucleating agents found in the literature are summarized in Table 6.

Only an overview is given, with nucleating agents which reduce supercooling by more than 50% of the initial value. Because supercooling is influenced by many factors, as detailed in part 2.2, the supercooling reduction will be considered, according to Eq 11.

$$Supercooling\ reduction\ (\%) = 100 \times (\Delta T_{without\ addtives} - \Delta T_{with\ additives})/\Delta T_{without\ addtives} \quad \text{Eq 11}$$

Some studies show low supercooling degrees after an additive has been used [60–63]. However, because of a lack of data on the supercooling degree of the pure materials, they could not be presented here as no supercooling reduction can be calculated. Table 6 also gives values which have an influence on supercooling with additives, such as nucleating agent size [44], when available, and proportion. The values taken for supercooling calculation were preferentially the onset of melting and freezing because peak values are heating and cooling rate dependent [64]. Studies have also been performed by adding nucleating agents to eutectic PCM [12,23,65–74], where at least two components have a concentration higher than 10% by weight.

Table 6 List of the nucleating agents and their effect on supercooling and latent heat, for different PCMs

PCM	Additives	wt% additive	Supercooling reduction (%)	Ref.
$CaCl_2.6H_2O$ Isomorphous	$BaI_2.6H_2O$	0.5	100.0	[12]
	K_2CO_3	0.5	50.0	[75]
	$SrCl_2.6H_2O$	0.1	58.2	[12]
		0.5	72.4	[12]
		1	100.0	[12]
		1	83.3	[75]
	$SrBr_2.6H_2O$	1	90.7	[75]
$CaCl_2.6H_2O$ Non isostructural	$BaCl_2$	0.01	88.2	[12]
		0.1	91.6	[12]
		0.5	100.0	[12]
	$BaCO_3$	0.5	100.0	[12]
		0.5	50.0	[75]
	BaO	0.1	97.5	[12]
	$Ba(OH)_2$	0.01	84.0	[12]
		0.05	94.1	[12]
		0.1	98.3	[12]
	$BaSO_4$	0.1	98.3	[12]
	$Sr(OH)_2$	0.5	100.0	[12]
$KF.4H_2O$	SiO_2		51.3	[76]
$LiNO_3{\cdot}3H_2O$	$Cu_3(OH)_5(NO_3).2H_2O$	0.1	87	[77]

Isomorphous		1	89	[77]
		2	90	[77]
		5	90	[77]
	$Zn(NO_3)_22[Zn(OH)_2]$	0.5	67	[77]
		0.9	69	[77]
		2.2	77	[77]
		4.2	84	[77]
$MgCl_2.6H_2O$ Isomorphous	$CaC_2O_4.H_2O$	0.5	100.0	[12]
	$CaK_2(SO_4)_2.H_2O$	0.5	51.5	[12]
	Na_3AIF_6	0.5	91.9	[12]
$MgCl_2.6H_2O$ Non isostructural	$Ba(OH)_2$	0.5	100.0	[12]
	BaO	0.5	99.0	[12]
	$Ca(OH)_2$	0.5	97.0	[12]
	CaO	0.5	100.0	[12]
		0.5	54.7	[78]
		1	44.7	[78]
		1.5	40.6	[78]
		2	43	[78]
		3	69.4	[78]
	$LiOH.H_2O$	1	50.0	[78]
	$Mg(OH)_2$	0.5	99.0	[12]
		2	59.8	[79]
		3	56.5	[79]
	$Sr(OH)_2$	0.5	100.0	[12]
		0.5	88.3	[79]
		1	85.9	[79]
		2	99.7	[79]
		0.5	49.4	[78]
		1	91.9	[78]
		1.5	43.3	[78]
		2	18.7	[78]
		3	100.0	[78]
	$SrCO_3$	0.5	100.0	[12]
		0.5	61.4	[79]
		1	82.6	[79]
		2	95.1	[79]
		3	96.7	[79]
		1.5	56.4	[78]
		2	84.7	[78]
		3	95.3	[78]
$Mg(NO_3)_2.6H_2O$ Isomorphous	$CaSO_4.2H_2O$	0.5	91.0	[12]
	$CoSO_4.4H_2O$	0.5	90.1	[12]
	$CuNa_2(SO_4)_2.2H_2O$	0.5	82.9	[12]
	$CuSO_4.3H_2O$	0.5	95.5	[12]
	$MgSO_4.4H_2O$	0.5	100.0	[12]
	$NaBO_2.2H_2O$	0.5	95.5	[12]
	$NiSO_4.4H_2O$	0.5	91.9	[12]
	$ZnSO_4.4H_2O$	0.5	74.8	[12]
$Mg(NO_3)_2.6H_2O$ Non isostructural	AlO(OH)	1	61.1	[80]
	$BaCO_3$	0.1	99.0	[12]
	BaO	0.1	100.0	[12]
		0.5	83.7	[80]

		1	88.4	[80]
		2	73.5	[80]
	BaO_2	1	92.3	[80]
	BaF_2	0.1	59.1	[12]
	$BaHPO_4$	0.1	50.9	[12]
	$Ba(OH)_2.8H_2O$	0.5	75.6	[80]
		1	89.1	[80]
		2	64.0	[80]
	$BaSO_4$	0.1	54.5	[12]
	$CaCO_3$	0.1	100.0	[12]
	CaO	0.1	100.0	[12]
		1	74.7	[80]
	$Ca(OH)_2$	0.1	100.0	[12]
		1	78.9	[80]
	$MgCO_3$	0.1	100.0	[12]
		1	83.5	[80]
	MgO	0.1	98.9	[12]
		0.5	89.4	[80]
		1	88.1	[80]
		2	78.4	[80]
	$Mg(OH)_2$	0.1	98.5	[12]
		0.5	87.6	[80]
		1	88.1	[80]
		2	89.8	[80]
	$Mg_3(PO_4)_2$	0.1	76.4	[12]
	$Sr(OH)_2$	0.1	100.0	[12]
		0.5	88.7	[80]
		1	82.8	[80]
		2	74.2	[80]
	$SrCO_3$	0.1	100.0	[12]
$NaCH_3COO.3H_2O$	8% KCl + $\alpha.Al_2O_3$ (100 nm)	2	68.2	[81]
	AlN (50 nm)	3	85.9	[82]
		4	94.1	[82]
	KCl	2	67.5	[81]
		4	87.6	[81]
		6	89.0	[81]
	K_2SO_4	1	95.0	[83]
	$Na_4P_2O_7.10H_2O$	0.5	90.3	[61]
		1	96.7	[83]
$Na_2HPO_4.12H_2O$	Al (8.5-20 µm)	3.7	67.5	[83]
	C (1.5-6.7 µm)	3.7	97.5	[83]
	Cu (1.5-2.5 µm)	3.7	96.3	[83]
	$Na_2B_4O_7.10H_2O$	2.9	62.5	[83]
	TiO_2 (2-200 µm)	3.7	97.5	[83]
$Na_2SO_4.10H_2O$	C	0.05	81.6	[84]
	$Na_2B_4O_7.10H_2O$	1.9	78.8	[83]
		0.02	97.8	[84]
			78.6	[76]
$Na_2S_2O_3.5H_2O$	C (1.5-6.7 µm)	3	72.5	[83]
	Na_2SO_4	2	75.0	[83]
	$SrSO_4$	5	95.0	[83]
$C_4H_{10}O_4$	bicyclic [2,2,1] heptane di-carboxylate	1	57.3	[85]
	$C_7H_{10}CaO_4$	1	64.5	[85]

	Calcium salt of benzene- 1, 3, 5-tricarboxylic acid	1	52.7	[85]
$C(CH_2OH)_4$	Nano AlN (50 nm)	3	76	[86]

Figure 11 presents the studies varying the percentage by weight of additives in the sample, and the effect of this variation on the supercooling reduction, for different salt hydrates.

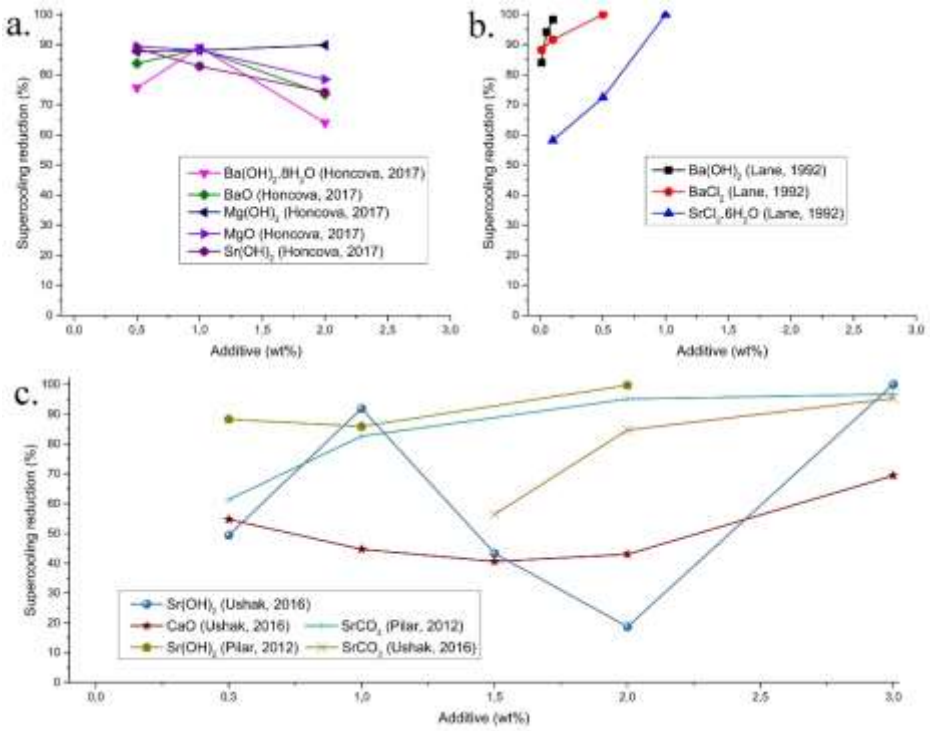

Figure 11 Evolution of the supercooling reduction for different PCMs, proportion, and types of additives. a. $Mg(NO_3)_2.6H_2O$; b. $CaCl_2.6H_2O$; c. $MgCl_2.6H_2O$. (Two columns image)

From Figure 11, no trend is clearly identified for the reduction of supercooling. Indeed, an increase in the proportion of the additive should decrease the supercooling, but new effects are appearing after a certain quantity of nucleating agents was introduced in the PCM, as suggested by [60]. In addition to these results, Figure 12 presents the average quantity (in percentage by weight) of different additives, which reduces supercooling by more than 90%. It is seen that the average quantity is around 1 wt% except for Borax ($Na_2B_4O_7.10H_2O$), where the quantity is more than 2 wt%.

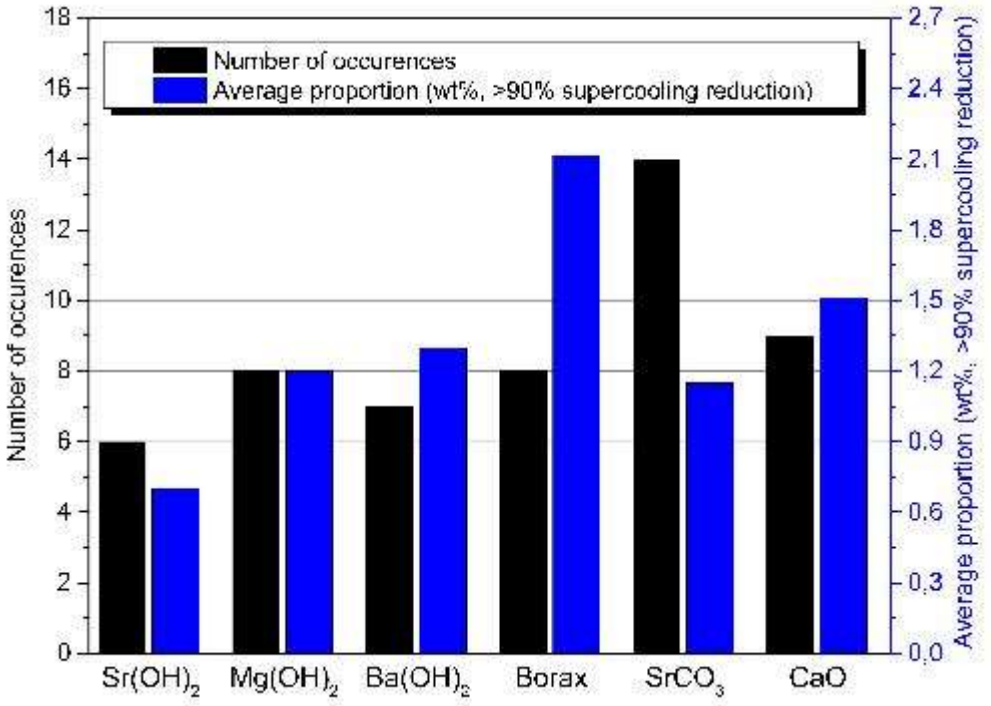

Figure 12 Number of studies where the additives have been used (considered only where more than five occurrences were noticed) and average proportion to decrease supercooling by more than 90%. NB: Borax: $Na_2B_4O_7.10H_2O$ (Single column image)

About the rule given by Telkes [58], previously described in Table 5, accurate studies were made to compare the nucleating agents with a crystalline structure close to the material they nucleate (within a 15% range) with the others, known as "non-isostructural". Results are illustrated in Figure 13, with the isomorphous material given in dark colors, and the non-isostructural material in a lighter color.

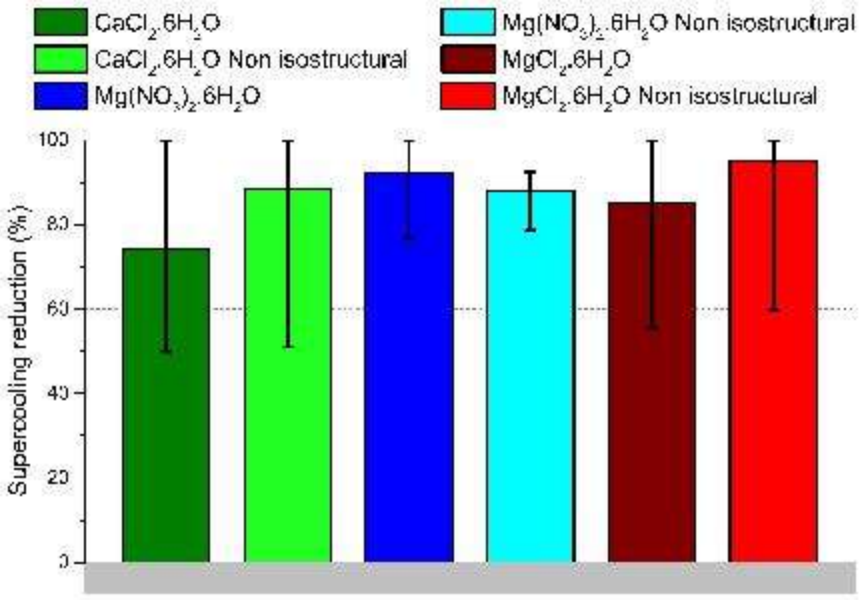

Figure 13 Effect of isomorphous and non-isostructural nucleating agents on the supercooling reduction. (Single column image)

As a conclusion, numerous nucleating agents are effective in the supercooling reduction from Table 6. Despite the fact that some of them can be used for different supercooled PCMs, they are more or less reliable depending on the material they try to solidify. This implies to test a large number of nucleating agent for each PCM needed to be solidified. This is clearly time-consuming and Table 6 is here to give some help in this task. Besides, when selecting a specific PCM, its effect is dependent on the percentage of additive added. The supercooling reduction versus additive quantity results in a nonlinear trend as some particular and unwanted effects take place at high percentages. An intermediate concentration such as 1wt% seems to be the most effective. Finally, the efficiency of a couple PCM-nucleating agent restricted to the "15% rule" as proposed by Telkes [58] is not so applicable in this context. Indeed, the error bars presented in Figure 13 does not allow for a clear discrimination between the two types of nucleating agent effects.

The interest in using nucleating agents for microencapsulated PCMs is also appearing to be a critical issue. Contrary to the bulk volume case where the liquid can be solidified from one nucleation site, emulsion and encapsulation divide the PCM sample into microscopic parts, isolated from each other, as explained by Günther [18]. Indeed, when the volume is lowered as in encapsulation techniques, fewer impurities are present to act as nucleating agents to reduce supercooling degree. Therefore, adding nucleating agents in the microcapsules composition allows the material to nucleate at a temperature comparable to that of the bulk volume.

4.2. Electrical means

Since the first experiment on electrofreezing was performed centuries ago [87], the phenomenon responsible for the nucleation of supercooled water under electric fields is not fully understood, due to a contribution of numerous effects. After that, in the period from 1950 to 1975, the studies were focused on water supercooling in clouds, and more recently in heat storage with PCM materials. Accurate experiments were first performed by Rau [88], which showed the appearance of ice nucleation under electric fields. To do so, millimeter-size water droplets were put between a polished chromium electrode and a glassy sphere, with about 0.5-3 kV (20-60 kV/cm) voltage to produce an electric field. It was able to trigger electrofreezing in water drop with only 4 K supercooling. It was assumed that electrofreezing gave specific orientations to water molecules, because of their polarity, and this process could induce freezing [89]. This hypothesis was discussed by Blanchard [90], who suggested that ice crystals were presents in the lab atmosphere and acted as seeding for the water drop. Some authors [91,92] also suggested that nucleation was due to electrical discharges. However, this cannot be a reproducible effect, according to Pruppacher [93,94], who analyzed the influence of electric field intensity and wall material on electrofreezing. He showed that supercooled water drops between two chromium electrodes, immersed in oil, can freeze water at 4 K supercooling with an electric field up to 30 kV/cm, without electrical discharge (the water could supercool below 260 K without electric fields). Later, he also performed some experiments where he reduced supercooling from 20 K to 8 K using a cloud made of sulfur particles [93]. Roulleau et al. [95] showed that a clean wire, electrically charged to a potential of 8 kV, in contact with the supercooled cloud, would not produce ice until a temperature of 253 K is reached. However, ice would be avoided when a hydrophobic material is used to cover the wire. Abbas et al. [96] studied the influence of different configurations, using mechanical or electrical devices, on the probability of freezing events. The authors were able to show this influence on both the probability of freezing and its temperature. Then Smith et al. [91] developed an experiment to reproduce the events occurring in supercooled clouds with water falling through it. It was shown that a sufficiently high value of the electric field would divide the bubble, followed by its freezing for a temperature below 267 K, confirming the conclusion from their previous publication [96]. In this paper, it was suggested that a bubble was appearing and collapsing during the bubble division, causing a cavitation effect in the material, which can be

responsible for a nucleation effect according to Hickling [97]. A relevant method for supercooled water electrofreezing was also purposed by Braslavsky et al. [98].

Mandal et al. [92] studied the effect of electrical discharge on the electrofreezing effect. It was observed that freezing can be triggered by electrical discharge when wires were used as electrodes, for a voltage of 6 kV. With this configuration, only 32% of the runs resulted in freezing. Besides, when the voltage was lowered to about 2.5 kV, or when the wire electrodes were replaced by spheres, no nucleation occurred.

Later, Shichiri et al. [99] studied the effect of different electrodes immersed in supercooled water. It was shown that supercooling was always reduced when a direct current was applied, compared to the no-current experiment. The impact of the electrode material on the freezing frequency on the anode or cathode was also investigated. It was observed that ionization tendency was related to nucleation probability on cathode or anode In a second paper [100], the investigation was made on the impact of both direct current, alternating current and electrostatic field on the freezing ability. Indeed, when a current was applied, H2 and O2 gas bubbles were formed by an electrolysis on the surface of the electrodes and that bigger bubbles were produced by an application of a DC current than for an AC current. A longer application would also increase bubble size. These bubbles, by leaving the surface, crystallized the surrounding liquid. It was guessed by the authors that a small region of the bubbles would gather water molecules because of a higher electrical charge density. This concentration would induce a higher supersaturation, nucleation would start inside the bubble from the electrode surface and continue its growth after the bubble left. This effect was magnified under direct current because these bubbles could grow continuously whereas AC and electrostatic field had low or no effect on it. A further investigation of the electrode material effect was made by Hozumi et al. [101], who measured the probability of a nucleation event for different electrode materials and different supercooling. He went further on nucleation's origin by assuming nucleation probability depends on the O-O link size in the ion formed in the supercooled liquid, saying that nucleation will increase if the O-O distance in the ion is similar to the O-O distance in ice. The different electrode material efficiencies are presented in Table 7, where the most effective electrodes seem to be Copper, Silver, Gold, and Aluminum.

Table 7 Electrode material efficiencies

Material	Electrode preference (nucleation probability, %)	Ref
Water	Pt (50%) > Ti (37%)	[99]
Water	Cu = Al (100%) > Ag (60%) > Au (31%) > Pt (10%) > C (0%)	[101]
$C_{16}H_{36}BrN$	Cu (100%) > Au (30%) > Fe (45%) > Ni = Al (0%)	[102]
$CH_3COONa.3H_2O$	Cu (10%) > Al = Au (0%)	[102]
$Na_2SO_4.10H_2O$	Au (40%) > Al (30%) > Cu (10%)	[102]

The volume studied must also be considered. Whereas the first studies use small volumes such as water droplets, subsequent studies have bigger volumes where the heterogeneous nucleation instead of the homogeneous could take place.

Studies on PCMs appeared later with Ohachi et al. [103], who observed nucleation of SAT with Cu electrode for different voltages and current values and the influence of water addition on solidification behavior was also analyzed. This work was pursued in a second paper [104] several years later, where the effect of the addition of NaOH on the induction time for electrical nucleation of SAT was studied. Another work was produced by Munakata et al. [105] on SAT where the nuclei position is shown, and the growth rate of this nuclei is measured. A study on erythritol has also been performed [106], where aluminum electrodes were immersed in supercooled liquid, linked to a 1 kV_{DC} power supply. The authors showed that, depending on the supercooling degree, nucleation could occur on electrode surfaces or on the vial edges. Kumano et al. [102] carried out a study on $C_{16}H_{36}BrN$ (TBAB) hydrates, $Na_2SO_4.10H_2O$ and $CH_3COONa.3H_2O$ testing different concentrations, electrode materials, voltage,

and supercooling degrees. It was observed that Cu electrodes were the most effective, particularly with TBAB hydrate samples.

All the experimental conditions from the previous paper can be summarized in Table 8. After years, the energy required to trigger nucleation decreases as the sample volume increases.

Table 8 Experiments performed with an electric device as the triggering technique

Current type	Voltage (V)	Electrode material	Sample volume (mm^3)	Sample material	Supercooling reduction (%)	Ref
DC	0 - 30000	Cr/$(C_2H_4)_n$, $(C_2F_4)_n$, $(C_5O_2H_8)_n$, $(C_2H_3Cl)_n$	4-8	H_2O	60	[94]
DC	0 - 8000	Pt (covered with vaseline, silicone oil, paraffin oil, paraffin wax, naphthalene, dodecane, phloroglucinol dihydrate	N/A	H_2O	75	[95]
DC	0 - 30000	Cu	5-10	H_2O	83	[96]
DC	0 - 30000	Cu-Zn	35-50	H_2O	50	[91]
DC	0 - 8000	W	N/A	H_2O	100	[92]
DC	0 - 1000	Mg, Al, Ti, Zr, Co, Ni, Cu, Ag, Pt, Au	105	H_2O	100	[99]
AC/DC	0 – 1000	Pt, Ti	105	H_2O	83	[100]
DC	0 - 50	Ag, Al, Au, C, Cu, Pt	4000	H_2O	60	[101]
DC	0 - 20	Cu, Al, Ni, Fe, Au	3000	$C_{16}H_{36}BrN$	100	[102]
AC/DC	(-2) - 1	Cu-amalgam	N/A	$CH_3COONa.3H_2O$	89	[103]
N/A	0 - 0.5	Ag, Pt	N/A	$CH_3COONa.3H_2O$	42	[104]
DC	0 - 1.5	Cu	3500	$CH_3COONa.3H_2O$	N/A	[105]
DC	0 - 1000	Ag	7250	$C_4H_{10}O_4$	54	[106]

4.3. Mechanical means

4.3.1. Dynamic high pressure

The first study of nucleation triggered by mechanical shock was performed by Young et al. [107] where the effect of both stirring and impact stress was studied. To do so, several substances were studied: water, benzene or PCM such as calcium chloride hexahydrate. After the material was cooled down to the desired temperature, a hammer was dropped with a certain energy, and the minimum supercooling degree for crystallization appearance was recorded. Figure 14 shows the effect of shock strength increase on supercooling temperature decrease. This was completed by a second study [108], to optimize the impact device and produce a relation between the impact energy and the supercooling reduction for water.

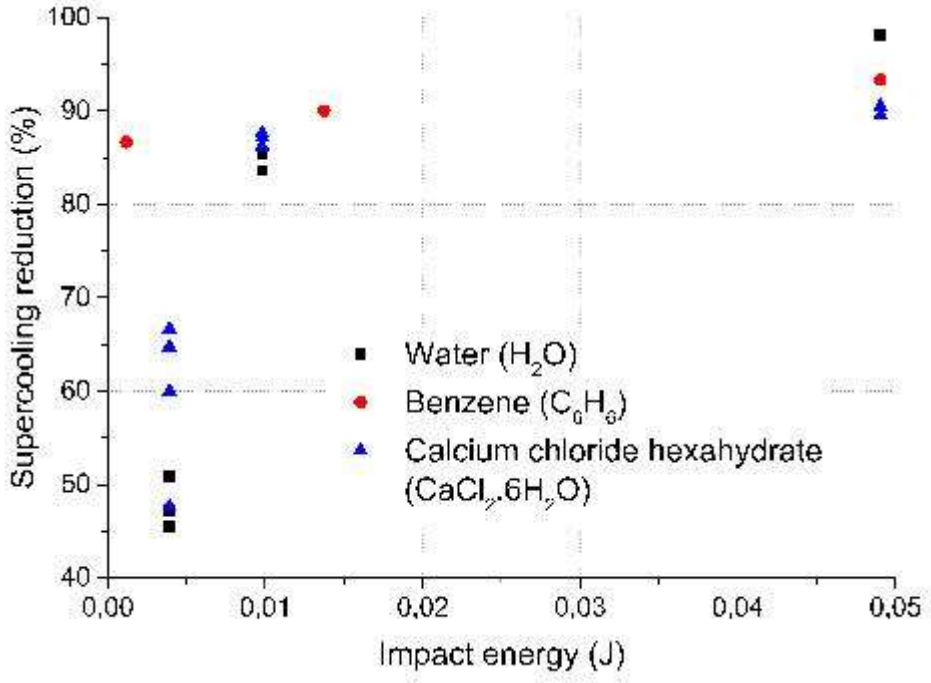

Figure 14 Supercooling evolution with the increase of impact energy, adapted from [107]. (Single column image)

From this study, the supercooling degree could be continuously reduced with an increase of the energy from the hammer. Indeed, it was reduced by more than 50% with a low (0,005J) impact energy, then reduced by 85% with an energy of 0.01J and close to 100% when the energy is up to 0.05J. The effect of mechanical shock was also independent of the material.

Another way of triggering nucleation by dynamic pressure is known as cavitation, where a high pressure is applied locally by a bubble collapse. However, the effect of cavitation on nucleation is not perfectly understood. As studied [109], the nucleation can be due to the pressure variation, as seen previously. This pressure can be applied macroscopically or microscopically as the cavitation process. As presented by Chalmers [45], there is, in cavitation, a competition between two phenomena:

- After a bubble collapse, a high pressure is induced. This pressure is sufficient to increase the melting point and produce homogeneous nucleation
- The evaporation from cavitation effect decreases the pressure of the bubble's surface to a temperature so low that homogeneous nucleation takes place.

These two processes have been discussed in the following years for water freezing, particularly by Hickling [97] and Hunt and Jackson [110] who supported the first hypothesis. These authors made their analysis considering water and it was assumed that, during the collapse of a bubble, a pressure wave is generated for a short time. According to the water phase diagram, the liquid will reach temperature and pressure points that are sufficient to turn it into solid. However, these authors' theories differ on the event where nucleation occurred: Hickling showed that solidification was provoked by an increase of pressure following the collapse of the bubble, calculated by [111], whereas Hunt and Jackson suggested that it was initiated by the following depression. If during this time of pressure change, the crystal growth rate is sufficient to reach its critical size, the solid will subsist after the pressure collapsed. It will then act as a seed crystal and will solidify the surrounding supercooled water.

Hickling [97] also assumed that some material could not be solidified by cavitation, because of a different phase diagram. For example, with Bismuth, the pressure required to turn the material into solid is higher than usual cavitation pressure. This assumption was used to explain the absence of nucleation by cavitation in PCMs such as salt hydrates [112,113]. The conclusion was that high pressure was not long enough for the crystal to reach its critical size. However, after some experiments on gallium [114], the theory developed by Hickling is not completely relevant and another theory of nucleation for supercooled melt should be used [110]. In this model, it was supposed that materials that expand on freezing will nucleate during the positive pressure period, whereas materials, like water, contract on freezing and will nucleate during the negative pressure period.

Cavitation, starting from a depression point, may have different origins: high-speed fluid flow (hydraulic cavitation) [115], ultrasonic irradiation (acoustic cavitation) [111], intense focused laser pulse (optic cavitation) [116]. The light emittance produced by acoustic pressure, called sonoluminescence, was discovered by Frenzel et al. [117] and was used for experimental cavitation detection [118,119].

In acoustic pressure, the sound wave created by a sonotrode produces positive and negative high pressure, with bubbles appearing with the depression wave. When a bubble collapses, a very high-pressure shockwave is applied for a short time. When a nucleus is able to reach its critical size within this time, it becomes stable and this stability increases with increasing size (if not, the nuclei disappear). Sononucleation is, therefore, dependent on the solid growth rate, time for high-pressure application and nuclei critical size [97].

Ultrasonic irradiation is often used to trigger nucleation of Phase Change Materials and several studies have been performed on different materials (water, salt hydrates, sugar alcohols), as reported in Table 9.

Table 9 Experiments performed with an ultrasonic device as triggering technique

US power (W)	US frequency (kHz)	US duration (s)	Sample material	Sample volume ($x10^3$ mm^3)	Supercooling reduction (%)	Ref.
0.13 W/cm²	0 – 1000	N/A	H_2O	1	30	[120]
N/A	27	0.022	H_2O	10	56	[121]
40	36	1	H_2O	3	62	[122]
100	39	5	H_2O	3600	70	[123]
180	20	4000	H_2O	100	71	[124]
100	20	N/A	H_2O	8	85	[37]
N/A	20	4000	K_2SO_4	200	30	[125]
50	20	60	$CH_3COONa.3H_2O$	17	89	[126]
50	20	90	$Na_2HPO_4.12H_2O$	50	100	[127]

Ultrasonic irradiation for water freezing has already been summarized by some authors [48,128]. From Table 9, it seems that nucleation ability is not only dependent on US power, duration of insonication or volume. A frequency of 20 kHz shows the best results, but it is also the most used value for these studies.

It was observed that the nucleation process with ultrasound was due to cavitation more than generated agitation [129]. The effect of agitation or ultrasonic irradiation on fracture of big crystals has also been observed [130]. It was proven by a microscopic study, performed by Chow et al. [131–133] that ice nucleation happens at the location where the bubble collapses.

Studies have also been performed to understand the effect of ultrasound on induction time (i.e. time from the start of ultrasonic irradiation to the appearance of the first crystal), on water [123,124,134], salt hydrates [125,126,135–137] or sugar alcohols [138]. The time for heat release (recalescence) is also improved by ultrasonic irradiation [51,139,140], where the influence of a large number of ultrasonic parameters was studied. The choice of the solvent also appears to be critical for the efficiency of crystallization triggered by ultrasound [141].

Some studies have also been performed on water and PCMs to determine how the final crystal size can be influenced by ultrasonic irradiation. Studies performed with different materials (water or PCM) showed that an increase of acoustic pressure (ultrasonic power) can decrease the particle size [122,142,143] because crystals are eroded or broken by the agitation produced by the ultrasonic wave. It was also found that ice crystal size decreases with an increase of supercooling [122,142] or oxygen content dissolved in the material [144]. Sonication often provides all the benefit of seeding on crystal size (short induction time, particle size distribution) without drawbacks such as handling or optimal moment determination for seeding [145]. Besides, a bigger volume of sample is known to increase the crystal size [145]. Crystal size does not seem to be influenced by the change of US frequency, from 15 kHz to 30 kHz [145].

Some experiments also show some difficulties in PCM nucleation triggering by ultrasound. No supercooling degree variation between the spontaneous case and sonication case was detected by Günther et al. [37,50] which is possibly explained by Rogerson et al.'s theoretical model [112,113].

It was found that induction time could be decreased with sufficient ultrasonic power [125,135,137], where the nucleation appears at lower supersaturation degree, the induction time is shortened by an increase in ultrasonic power [139]. The crystal appearance probability was dependent on several parameters such as the supercooling degree before sonication [122,126], ultrasonic power [124,126,139,145], an excess of water in hydrated salts [126], the size of the probe [145], the immersion depth of probe [145], the test tube material [146], or the number of bubble nuclei [134]. A model was also developed by Zhang [134] to simulate the nucleation by ultrasound, and correlated with an experimental study on ice. An XRD characterization after solidification by ultrasonic irradiation showed a crystal structure with no difference to the initial one [135].

Studies were performed by Hozumi et al. [120,147], which showed that using an immersed steel bar to produce ultrasonic irradiation was much more efficient than using an external transducer. Because the first crystal appears on the steel surface, it is possibly working as a substrate for heterogeneous nucleation. Therefore, Wei et al [136] used an external ultrasonic probe to trigger nucleation in a PCM, resulting in a longer induction time. Indeed, the ultrasonic power arriving in the sample is much lower compared to the intrusive one [148]. Some accurate experimental benches have also been designed to study the solidification of ice clearly by using external ultrasonic irradiation, such as the one developed by Montes Quiroz [146].

One of the major problems in a solidification study is to avoid external nucleation sites such as the container wall, where nucleation might be stimulated. This could be solved by homogeneous solidification where nucleation ability is dependent on the material only, and not on any external factor.

One way to produce homogeneous nucleation is to make a bubble levitate in a containerless environment, to measure the exact ability of any material to nucleate by ultrasonic irradiation. One of the first uses of a levitating bubble to nucleate ice was performed by Ohsaka [149], where supercooling was reduced from 12 K to 5 K thanks to the cavitation effect. A second study by Chow et al [121] also showed that supercooling was reduced from 9 K to 3.5 K using ultrasound and cavitation. The bubble also has the possibility to move and collapse in several places under ultrasonic irradiation, nucleating crystals at different positions [121], in contradiction with the work of Ohsaka. A study

performed by Lü et al. [150] on levitating bubbles in supercooled water tends to show that the nucleation rate increases with an increased sound pressure level or an increased drop surface. A second study [151] on PCMs (aqueous KCl and NaCl) showed a relevant reduction of supercooling, from 47.5 K to 20.6 K for NaCl and from 47 K to 16.7 K for KCl, when an acoustic pressure was applied to a levitating bubble.

Because it produces a homogeneous nucleation event, a levitating bubble device was used for a better understanding of classical nucleation theory [152] by measuring the energy required for ice nucleation, depending on supercooling.

4.3.2. Agitation

The process of nucleation by agitation is not really well known. This effect is sometimes significant and can reduce supercooling of salt hydrates [153,154]. However, the process is not clearly understood and seems to be a competition of different effects:

- The decrease of supercooling at low agitation;
- The increase of supercooling is possible at medium agitation speed, possibly due to erosion into crystals smaller than the critical radius, which reduces the primary nucleation effect;
- The decrease of supercooling at a high agitation rate because of a possible growth of crystals from secondary nucleation.

This competition of effects can be illustrated as shown in Figure 15.

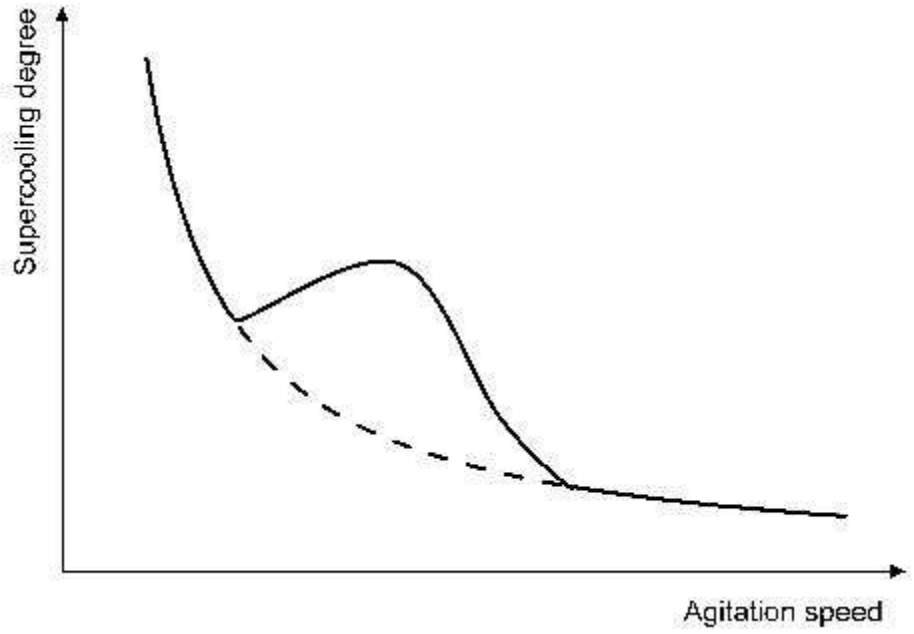

Figure 15 Supercooling degree versus agitation speed. Dashed line: diffusion effect. Continuous line: the combination of diffusion and attrition effect. Reprinted from [47], Copyright 2001, with permission from Elsevier. (Single column image)

A recent study shows that time and temperature of agitation have an influence on the solidification and the final crystal size of calcium sulfate [155].

4.4. Solidification technique comparison

A summary of the different techniques previously presented is given in Table 10.

Table 10 Techniques comparison

Method	Heat release control	Most favorable parameters supercooling reduction >90%	Limits
Seeding	Yes	Most reproducible technique	Keep some materials solid during heating step [54,55]
Nucleating agents	No	1wt% of additives Most effective: $Sr(OH)_2$, $Mg(OH)_2$, $Ba(OH)_2$, $SrCO_3$, CaO, $Na_2B_4O_7.10H_2O$	No control of heat release
Electrical	Yes	Use of Cu [101,102], or Ag [101] electrodes Use of direct current [92,99,102]	Voltage is dependent on volume Electrode may act as heterogeneous nucleation site
Mechanical shock	Yes	Impact force higher than 0.015 J [107]	
Ultrasound	Yes	A frequency of 20 kHz [127] Use an immersed probe [120,127] Insulate the material from the ambient air [120]	An immersed probe may act as a heterogeneous nucleation site
Agitation	Yes	High agitation rate [154]	Crystal erosion effect have to be avoided

From Table 10, some techniques are mature and can lead to the development of applications, such as seeding. Additives are a good alternative whereas heat release onset cannot be controlled. Solidification by electrical, mechanical or US irradiation means allows for heat release control, but the most favorable parameters have been less studied and are still under research.

4.5. Application using controlled nucleation from a supercooled liquid

Several applications have been developed for the thermal energy storage, where the supercooling phenomenon was suppressed by the different methods presented above as the well-known reusable heat pack produced by numerous companies. Heat could be stored under the supercooled state by this pack with no spontaneous solidification. This has led to other applications such as the one developed by Desgrosseillers [156] for daily storage. The fabricated device was able to store 0.3 kWh of heat within 7 h in a 1.6 L module [13], where springs were used as triggering devices, trapping crystals during the melting step and releasing them to trigger nucleation, as seen in Figure 16a. and 16b.

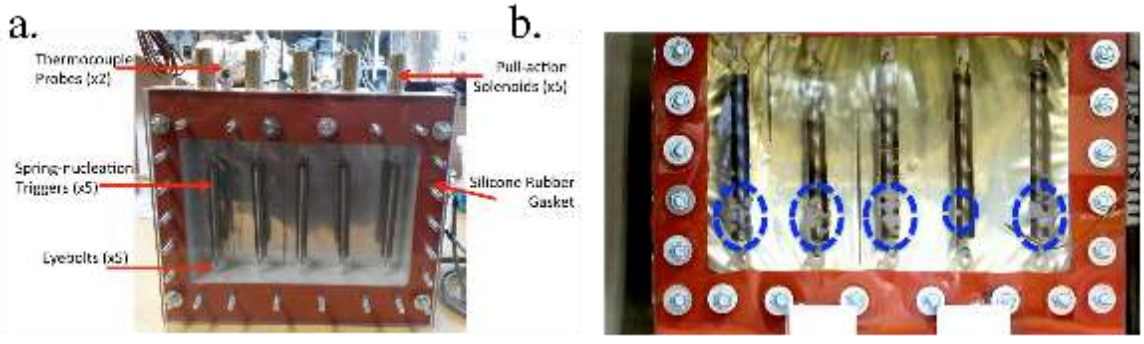

Figure 16 The triggering devices tested by Desgrosseillers [13] a) General presentation. b) Solidification step (crystals growing in the blue area). (Single column image)

Long-term energy storage can also be used to store the energy from the solar thermal panels. Dannemand et al [14] developed a storage device prototype composed of 24 modules containing each 250 L of salt-water mixture. The different modules could be supercooled for months and solidified by a seeding method when the heat was needed.

Another development using seeding technique was developed by H. M. Heizkörper GmbH [157]. A 150L tank was filled with 35 kg of a sodium acetate trihydrate – water mix. The phase change material could be kept under the supercooled state for days [158] and solidified by seeding when the desired temperature is reached.

Applications were also developed from nucleating agents. Sunamp developed a heat battery [159] containing 19L of sodium acetate trihydrate, able to release 2.5 kWh of heat. The material composition was improved with a polymer to avoid the latent heat decrease after cycles or DSP as nucleating agent [159].

For mechanical or electrical techniques, a lack of applications has been noted. This can be due to the contradictory results and the lower number of studies showing a good reduction of supercooling with these methods.

Applications in the automotive industry usually use PCMs for the preheating of the engine or of the catalytic converter. Huntemann et al. [160] presented a reduction of gas emission at cold start of the engine with a use of different salt hydrates: a eutectic salt or sodium acetate trihydrate, with tetrasodium pyrophosphate decahydrate as an additive to prevent supercooling phenomenon. The same target was pursued by Vasiliev et al [161] who used $NaOH \cdot H_2O$ with an unknown additive to reduce the gas emission of a bus.

5. Conclusion

A compilation of techniques was presented in this review, showing their ability to trigger solidification of water and PCMs, with their different pros and cons. Addition of nucleating agents was shown to be the most effective solution. Several additives, such as strontium hydroxide, allow for a reduction of supercooling by more than 90% with a low amount of material (1 wt%), preserving the high latent heat property of the material. This work aims to help in the preparation of a PCM by giving an overview of the PCM-additive combination presented to be efficient in supercooling reduction. Therefore, this method is reproducible and cheap because no particular device is required. As a consequence, interest in this method has grown over the past five years. However, there is no possibility of releasing heat on demand by using this technique as the heterogeneous solidification started when the material reached a temperature low enough.

The other techniques, such as ultrasonic wave or electric nucleation where the solidification is dynamically induced in the material, enable us to control the nucleation time when the heat is needed. They also influence the crystal's properties, such as its size. However, they are more difficult to develop as they require a specific type of facility. In addition to this, the energy needed to provoke electrofreezing in a small volume is particularly high: up to tens of kV for the freezing of a size drop smaller in milliliter range, avoiding applications in microencapsulated materials. They could be devoted to larger volumes where such a system could be more easily implemented. Further work also needs to be done to understand how the solidification is triggered by both techniques and to ensure the development of a reliable device.

Even though some interesting results may be obtained using these triggering techniques, this review does not consider several problems to which PCMs are subjected, such as aging. Indeed, salt hydrates suffer from segregation, particularly when they are kept supercooled for days. This segregation has to be considered, and the addition of thickening agents is a possible solution to decreasing the segregation effects, maintaining a large heat storage capacity after days.

6. References

[1] T.-C. Ling, C.-S. Poon, Use of phase change materials for thermal energy storage in concrete: An overview, Constr. Build. Mater. 46 (2013) 55–62. doi:10.1016/j.conbuildmat.2013.04.031.

[2] L.F. Cabeza, A. Castell, C. Barreneche, A. de Gracia, A.I. Fernández, Materials used as PCM in thermal energy storage in buildings: A review, Renew. Sustain. Energy Rev. 15 (2011) 1675–1695. doi:10.1016/j.rser.2010.11.018.

[3] A. Waqas, Z. Ud Din, Phase change material (PCM) storage for free cooling of buildings—A review, Renew. Sustain. Energy Rev. 18 (2013) 607–625. doi:10.1016/j.rser.2012.10.034.

[4] H. Akeiber, P. Nejat, M.Z.A. Majid, M.A. Wahid, F. Jomehzadeh, I. Zeynali Famileh, J.K. Calautit, B.R. Hughes, S.A. Zaki, A review on phase change material (PCM) for sustainable passive cooling in building envelopes, Renew. Sustain. Energy Rev. 60 (2016) 1470–1497. doi:10.1016/j.rser.2016.03.036.

[5] F. Souayfane, F. Fardoun, P.-H. Biwole, Phase change materials (PCM) for cooling applications in buildings: A review, Energy Build. 129 (2016) 396–431. doi:10.1016/j.enbuild.2016.04.006.

[6] B. Stutz, N. Le Pierres, F. Kuznik, K. Johannes, E. Palomo Del Barrio, J.-P. Bédécarrats, S. Gibout, P. Marty, L. Zalewski, J. Soto, N. Mazet, R. Olives, J.-J. Bezian, D.P. Minh, Storage of thermal solar energy, Comptes Rendus Phys. 18 (2017) 401–414. doi:10.1016/j.crhy.2017.09.008.

[7] N.R. Jankowski, F.P. McCluskey, A review of phase change materials for vehicle component thermal buffering, Appl. Energy. 113 (2014) 1525–1561. doi:10.1016/j.apenergy.2013.08.026.

[8] Z. Ling, Z. Zhang, G. Shi, X. Fang, L. Wang, X. Gao, Y. Fang, T. Xu, S. Wang, X. Liu, Review on thermal management systems using phase change materials for electronic components, Li-ion batteries and photovoltaic modules, Renew. Sustain. Energy Rev. 31 (2014) 427–438. doi:10.1016/j.rser.2013.12.017.

[9] S.K. Sahoo, M.K. Das, P. Rath, Application of TCE-PCM based heat sinks for cooling of electronic components: A review, Renew. Sustain. Energy Rev. 59 (2016) 550–582. doi:10.1016/j.rser.2015.12.238.

[10] C. Kinkelin, S. Lips, U. Soupremanien, V. Remondière, J. Dijon, H. Le Poche, E. Ollier, M. Zegaoui, N. Rolland, P.-A. Rolland, S. Lhostis, B. Descouts, Y. Kaplan, F. Lefèvre, Theoretical and experimental study of a thermal damper based on a CNT/PCM composite structure for transient electronic cooling, Energy Convers. Manag. 142 (2017) 257–271. doi:10.1016/j.enconman.2017.03.034.

[11] T. Adachi, D. Daudah, G. Tanaka, Effects of Supercooling Degree and Specimen Size on Supercooling Duration of Erythritol, ISIJ Int. 54 (2014) 2790–2795. doi:10.2355/isijinternational.54.2790.

[12] G.A. Lane, Phase change materials for energy storage nucleation to prevent supercooling, Sol. Energy Mater. Sol. Cells. 27 (1992) 135–160. doi:10.1016/0927-0248(92)90116-7.

[13] L. Desgrosseilliers, Design and Evaluation of a Modular, Supercooling Phase Change Heat Storage Device for Indoor Heating, Thesis, 2017. https://DalSpace.library.dal.ca/handle/10222/73309 (accessed January 30, 2018).

[14] M. Dannemand, W. Kong, J. Fan, J.B. Johansen, S. Furbo, Laboratory Test of a Prototype Heat Storage Module Based on Stable Supercooling of Sodium Acetate Trihydrate, Energy Procedia. 70 (2015) 172–181. doi:10.1016/j.egypro.2015.02.113.

[15] A. Abhat, Low temperature latent heat thermal energy storage: Heat storage materials, Sol. Energy. 30 (1983) 313–332. doi:10.1016/0038-092X(83)90186-X.

[16] B. Zalba, J.M. Marín, L.F. Cabeza, H. Mehling, Review on thermal energy storage with phase change: materials, heat transfer analysis and applications, Appl. Therm. Eng. 23 (2003) 251–283. doi:10.1016/S1359-4311(02)00192-8.
[17] L.F. Cabeza, A. Castell, C. Barreneche, A. de Gracia, A.I. Fernández, Materials used as PCM in thermal energy storage in buildings: A review, Renew. Sustain. Energy Rev. 15 (2011) 1675–1695. doi:10.1016/j.rser.2010.11.018.
[18] E. Günther, T. Schmid, H. Mehling, S. Hiebler, L. Huang, Subcooling in hexadecane emulsions, Int. J. Refrig. 33 (2010) 1605–1611. doi:10.1016/j.ijrefrig.2010.07.022.
[19] T.U. Schülli, R. Daudin, G. Renaud, A. Vaysset, O. Geaymond, A. Pasturel, Substrate-enhanced supercooling in AuSi eutectic droplets, Nature. 464 (2010) 1174–1177. doi:10.1038/nature08986.
[20] M. Faucheux, G. Muller, M. Havet, A. LeBail, Influence of surface roughness on the supercooling degree: Case of selected water/ethanol solutions frozen on aluminium surfaces, Int. J. Refrig. 29 (2006) 1218–1224. doi:10.1016/j.ijrefrig.2006.01.002.
[21] S. Puupponen, A. Seppälä, Cold-crystallization of polyelectrolyte absorbed polyol for long-term thermal energy storage, Sol. Energy Mater. Sol. Cells. 180 (2018) 59–66. doi:10.1016/j.solmat.2018.02.013.
[22] A. Mollova, R. Androsch, D. Mileva, C. Schick, A. Benhamida, Effect of Supercooling on Crystallization of Polyamide 11, Macromolecules. 46 (2013) 828–835. doi:10.1021/ma302238r.
[23] Z. Zhang, Y. Yuan, N. Zhang, X. Cao, Thermophysical Properties of Some Fatty Acids/Surfactants as Phase Change Slurries for Thermal Energy Storage, J. Chem. Eng. Data. 60 (2015) 2495–2501. doi:10.1021/acs.jced.5b00371.
[24] Y. Konuklu, Microencapsulation of phase change material with poly(ethylacrylate) shell for thermal energy storage, Int. J. Energy Res. 38 (2014) 2019–2029. doi:10.1002/er.3216.
[25] A. Sari, Thermal energy storage properties of mannitol–fatty acid esters as novel organic solid–liquid phase change materials, Energy Convers. Manag. 64 (2012) 68–78. doi:10.1016/j.enconman.2012.07.003.
[26] H. Hidaka, M. Yamazaki, M. Yabe, H. Kakiuchi, E.P. Ona, Y. Kojima, H. Matsuda, Evaluation of fundamental characteristics of D-Threitol as phase change material at high temperature, (n.d.) 6.
[27] A. Seppälä, A. Meriläinen, L. Wikström, P. Kauranen, The effect of additives on the speed of the crystallization front of xylitol with various degrees of supercooling, Exp. Therm. Fluid Sci. 34 (2010) 523–527. doi:10.1016/j.expthermflusci.2009.11.005.
[28] F. Roget, Définition, modélisation et validation expérimentale d'une capacité de stockage thermique par chaleur latente adaptée à une centrale thermodynamique solaire à basse température, PhD Thesis, Toulon, 2012.
[29] L. Carpentier, S. Desprez, M. Descamps, Crystallization and glass properties of pentitols, J. Therm. Anal. Calorim. 73 (2003) 577–586.
[30] M. Kumar Trivedi, A. Branton, Characterisation of Physical, Spectral and Thermal Properties of Biofield treated Resorcinol, Org. Chem. Curr. Res. 04 (2015). doi:10.4172/2161-0401.1000146.
[31] M.D. Ossowska-Chruściel, E. Juszyńska-Gałązka, W. Zając, A. Rudzki, J. Chruściel, Mesomorphic properties of resorcinol, J. Mol. Struct. 1082 (2015) 103–113. doi:10.1016/j.molstruc.2014.10.080.
[32] E. Palomo Del Barrio, R. Cadoret, J. Daranlot, F. Achchaq, New sugar alcohols mixtures for long-term thermal energy storage applications at temperatures between 70 °C and 100 °C, Sol. Energy Mater. Sol. Cells. 155 (2016) 454–468. doi:10.1016/j.solmat.2016.06.048.
[33] A. Paul, L. Shi, C.W. Bielawski, A eutectic mixture of galactitol and mannitol as a phase change material for latent heat storage, Energy Convers. Manag. 103 (2015) 139–146. doi:10.1016/j.enconman.2015.06.013.
[34] W. Kong, M. Dannemand, J.B. Johansen, J. Fan, J. Dragsted, G. Englmair, S. Furbo, Experimental investigations on heat content of supercooled sodium acetate trihydrate by a simple heat loss method, Sol. Energy. 139 (2016) 249–257. doi:10.1016/j.solener.2016.09.045.

[35] J. Schroder, K. Gawron, Heat storage material comprising lithium chlorate-trihydrate and a nucleating agent, 4189393, 1980. http://www.freepatentsonline.com/4189393.html (accessed March 12, 2018).
[36] G.A. Lane, Solar Heat Storage: Latent Heat Material, vol. II, Technology, CRC Press, 1986.
[37] E. Günther, Sononucleation of Inorganic Phase Change Materials, Technische Universität München, 2009.
[38] K. Nagano, T. Mochida, S. Takeda, R. Domański, M. Rebow, Thermal characteristics of manganese (II) nitrate hexahydrate as a phase change material for cooling systems, Appl. Therm. Eng. 23 (2003) 229–241. doi:10.1016/S1359-4311(02)00161-8.
[39] P.J. Shamberger, T. Reid, Thermophysical Properties of Lithium Nitrate Trihydrate from (253 to 353) K, J. Chem. Eng. Data. 57 (2012) 1404–1411. doi:10.1021/je3000469.
[40] A. Sharma, V.V. Tyagi, C.R. Chen, D. Buddhi, Review on thermal energy storage with phase change materials and applications, Renew. Sustain. Energy Rev. 13 (2009) 318–345. doi:10.1016/j.rser.2007.10.005.
[41] P. Pacák, Crystal growth from a calcium nitrate tetrahydrate melt, Krist. Tech. 15 (1980) 523–529. doi:10.1002/crat.19800150505.
[42] E.A. Dancy, The behavior of saturated solutions of trisodium phosphate dodecahydrate as heat storage media, Sol. Energy. 33 (1984) 41–48. doi:10.1016/0038-092X(84)90115-4.
[43] R. Naumann, H. Emons, Results of thermal analysis for investigation of salt hydrates as latent heat-storage materials, J. Therm. Anal. Calorim. 35 (1989) 1009–1031.
[44] Y. Ma, B. Lei, Y. Liu, T. Wu, Effects of additives on the subcooling behavior of Al2(SO4)3·18H2O phase transition, Appl. Therm. Eng. 99 (2016) 189–194. doi:10.1016/j.applthermaleng.2015.12.119.
[45] B. Chalmers, Principles of solidification., Wiley, New York, 1964.
[46] A. S. Myerson, Concluding remarks, Faraday Discuss. 179 (2015) 543–547. doi:10.1039/C5FD00042D.
[47] J.W. Mullin, 5 - Nucleation, in: Cryst. Fourth Ed., Butterworth-Heinemann, Oxford, 2001: pp. 181–215. doi:10.1016/B978-075064833-2/50007-3.
[48] M. Dalvi-Isfahan, N. Hamdami, E. Xanthakis, A. Le-Bail, Review on the control of ice nucleation by ultrasound waves, electric and magnetic fields, J. Food Eng. 195 (2017) 222–234. doi:10.1016/j.jfoodeng.2016.10.001.
[49] B. Sandnes, J. Rekstad, Supercooling salt hydrates: Stored enthalpy as a function of temperature, Sol. Energy. 80 (2006) 616–625. doi:10.1016/j.solener.2004.11.014.
[50] B. Sandnes, Exergy Efficient Production, Storage and Distribution of Solar Energy (Ph.D. Thesis), Ph.D. Thesis, University of Oslo, 2004.
[51] E.P. Ona, X. Zhang, S. Ozawa, H. Matsuda, H. Kakiuchi, M. Yabe, M. Yamazaki, M. Sato, Influence of Ultrasonic Irradiation on the Solidification Behavior of Erythritol as a PCM, J. Chem. Eng. Jpn. 35 (2002) 290–298. doi:10.1252/jcej.35.290.
[52] F. Simon, G. Glatzel, Bemerkungen zur Schmelzdruckkurve, Z. Für Anorg. Allg. Chem. 178 (1929) 309–316. doi:10.1002/zaac.19291780123.
[53] P.F. Barrett, L.M.A. Naykalyk, Determination of the high pressure melting points of salt hydrates, Mater. Chem. Phys. 21 (1989) 201–208. doi:10.1016/0254-0584(89)90114-4.
[54] A.E.M. Anthony, P.F. Barrett, B.K. Dunning, Verification of a mechanism for nucleating crystallization of supercooled liquids, Mater. Chem. Phys. 25 (1990) 199–205. doi:10.1016/0254-0584(90)90084-N.
[55] P.F. Barrett, D.K. Benson, A mechanism for nucleating supercooled liquids, Mater. Chem. Phys. 20 (1988) 171–178. doi:10.1016/0254-0584(88)90108-3.
[56] E. Günther, H. Mehling, M. Werner, Melting and nucleation temperatures of three salt hydrate phase change materials under static pressures up to 800 MPa, J. Phys. Appl. Phys. 40 (2007) 4636. doi:10.1088/0022-3727/40/15/042.
[57] B. Sandnes, The physics and the chemistry of the heat pad, Am. J. Phys. 76 (2008) 546–550. doi:10.1119/1.2830533.
[58] M. Telkes, Nucleation of supersaturated inorganic salt solutions, Ind. Eng. Chem. 44 (1952) 1308–1310.
[59] D. Turnbull, B. Vonnegut, Nucleation catalysis., Ind. Eng. Chem. 44 (1952) 1292–1298.

[60] M. Fashandi, S.N. Leung, Sodium acetate trihydrate-chitin nanowhisker nanocomposites with enhanced phase change performance for thermal energy storage, Sol. Energy Mater. Sol. Cells. 178 (2018) 259–265. doi:10.1016/j.solmat.2018.01.037.
[61] W. Cui, Y. Yuan, L. Sun, X. Cao, X. Yang, Experimental studies on the supercooling and melting/freezing characteristics of nano-copper/sodium acetate trihydrate composite phase change materials, Renew. Energy. 99 (2016) 1029–1037. doi:10.1016/j.renene.2016.08.001.
[62] Y. He, N. Zhang, Y. Yuan, X. Cao, L. Sun, Y. Song, Improvement of supercooling and thermal conductivity of the sodium acetate trihydrate for thermal energy storage with α-Fe2O3 as addictive, J. Therm. Anal. Calorim. 133 (2018) 859–867. doi:10.1007/s10973-018-7166-2.
[63] J. Mao, J. Li, G. Peng, J. Li, A Selection and Optimization Experimental Study of Additives to Thermal Energy Storage Material Sodium Acetate Trihydrate, in: 2009 Int. Conf. Energy Environ. Technol., 2009: pp. 14–17. doi:10.1109/ICEET.2009.11.
[64] X. Zhang, Y. Fan, X. Tao, K. Yick, Crystallization and prevention of supercooling of microencapsulated n-alkanes, J. Colloid Interface Sci. 281 (2005) 299–306. doi:10.1016/j.jcis.2004.08.046.
[65] K. Shahbaz, I.M. AlNashef, R.J.T. Lin, M.A. Hashim, F.S. Mjalli, M.M. Farid, A novel calcium chloride hexahydrate-based deep eutectic solvent as a phase change materials, Sol. Energy Mater. Sol. Cells. 155 (2016) 147–154. doi:10.1016/j.solmat.2016.06.004.
[66] F.Y. Zhu, H.X. Zhou, Y.Q. Zhou, H.W. Ge, W.C. Fang, Y. Fang, C.H. Fang, Phase change performance assessment of salt mixtures for thermal energy storage material, Int. J. Energy Res. (2017) n/a-n/a. doi:10.1002/er.3747.
[67] A. Efimova, S. Pinnau, M. Mischke, C. Breitkopf, M. Ruck, P. Schmidt, Development of salt hydrate eutectics as latent heat storage for air conditioning and cooling, Thermochim. Acta. 575 (2014) 276–278. doi:10.1016/j.tca.2013.11.011.
[68] Y. Wu, T. Wang, Hydrated salts/expanded graphite composite with high thermal conductivity as a shape-stabilized phase change material for thermal energy storage, Energy Convers. Manag. 101 (2015) 164–171. doi:10.1016/j.enconman.2015.05.006.
[69] Y. Wu, T. Wang, Preparation and characterization of hydrated salts/silica composite as shape-stabilized phase change material via sol–gel process, Thermochim. Acta. 591 (2014) 10–15. doi:10.1016/j.tca.2014.07.012.
[70] L. Zhang, J. Zhu, W. Zhou, J. Wang, Y. Wang, Thermal and electrical conductivity enhancement of graphite nanoplatelets on form-stable polyethylene glycol/polymethyl methacrylate composite phase change materials, Energy. 39 (2012) 294–302. doi:10.1016/j.energy.2012.01.011.
[71] Z. Ling, J. Liu, Q. Wang, W. Lin, X. Fang, Z. Zhang, MgCl2·6H2O-Mg(NO3)2·6H2O eutectic/SiO2 composite phase change material with improved thermal reliability and enhanced thermal conductivity, Sol. Energy Mater. Sol. Cells. 172 (2017) 195–201. doi:10.1016/j.solmat.2017.07.019.
[72] G. Diarce, I. Gandarias, Á. Campos-Celador, A. García-Romero, U.J. Griesser, Eutectic mixtures of sugar alcohols for thermal energy storage in the 50–90°C temperature range, Sol. Energy Mater. Sol. Cells. 134 (2015) 215–226. doi:10.1016/j.solmat.2014.11.050.
[73] Y.T. Li, D.J. Yan, Y.F. Guo, S.Q. Wang, T.L. Deng, Studies on Magnesium Chloride Hexahydrate as Phase Change Materials, Appl. Mech. Mater. 71–78 (2011) 2598–2601. doi:10.4028/www.scientific.net/AMM.71-78.2598.
[74] C. Li, H. Yu, Y. Song, M. Zhao, Synthesis and characterization of PEG/ZSM-5 composite phase change materials for latent heat storage, Renew. Energy. 121 (2018) 45–52. doi:10.1016/j.renene.2017.12.089.
[75] I.M. Sutjahja, S.R. A U, N. Kurniati, I.D. Pallitine, D. Kurnia, The role of chemical additives to the phase change process of $CaCl_2.6H_2O$ to optimize its performance as latent heat energy storage system, J. Phys. Conf. Ser. 739 (2016) 012064. doi:10.1088/1742-6596/739/1/012064.
[76] K. Gawron, J. Schröder, Properties of some salt hydrates for latent heat storage, Int. J. Energy Res. 1 (1977) 351–363. doi:10.1002/er.4440010407.
[77] P.J. Shamberger, M.J. O'Malley, Heterogeneous nucleation of thermal storage material LiNO3·3H2O from stable lattice-matched nucleation catalysts, Acta Mater. 84 (2015) 265–274. doi:10.1016/j.actamat.2014.10.051.

[78] S. Ushak, A. Gutierrez, C. Barreneche, A.I. Fernandez, M. Grágeda, L.F. Cabeza, Reduction of the subcooling of bischofite with the use of nucleatings agents, Sol. Energy Mater. Sol. Cells. 157 (2016) 1011–1018. doi:10.1016/j.solmat.2016.08.015.
[79] R. Pilar, L. Svoboda, P. Honcova, L. Oravova, Study of magnesium chloride hexahydrate as heat storage material, Thermochim. Acta. 546 (2012) 81–86. doi:10.1016/j.tca.2012.07.021.
[80] P. Honcova, R. Pilar, V. Danielik, P. Soska, G. Sadovska, D. Honc, Suppressing supercooling in magnesium nitrate hexahydrate and evaluating corrosion of aluminium alloy container for latent heat storage application, J. Therm. Anal. Calorim. 129 (2017) 1573–1581. doi:10.1007/s10973-017-6334-0.
[81] X. Li, Y. Zhou, H. Nian, F. Zhu, X. Ren, O. Dong, C. Hai, Y. Shen, J. Zeng, Preparation and thermal energy storage studies of CH3COONa·3H2O–KCl composites salt system with enhanced phase change performance, Appl. Therm. Eng. 102 (2016) 708–715. doi:10.1016/j.applthermaleng.2016.04.029.
[82] P. Hu, D.-J. Lu, X.-Y. Fan, X. Zhou, Z.-S. Chen, Phase change performance of sodium acetate trihydrate with AlN nanoparticles and CMC, Sol. Energy Mater. Sol. Cells. 95 (2011) 2645–2649. doi:10.1016/j.solmat.2011.05.025.
[83] H.W. Ryu, S.W. Woo, B.C. Shin, S.D. Kim, Prevention of supercooling and stabilization of inorganic salt hydrates as latent heat storage materials, Sol. Energy Mater. Sol. Cells. 27 (1992) 161–172. doi:10.1016/0927-0248(92)90117-8.
[84] C.-B. Leng, X. Ji, X. Luo, M. Li, Q.-F. Yu, Y.-F. Xu, Preparation and performance analysis of Na2SO4·10H2O/EG composite phase-change materials, Cailiao GongchengJournal Mater. Eng. 45 (2017) 58–64. doi:10.11868/j.issn.1001-4381.2015.000073.
[85] J.-L. Zeng, L. Zhou, Y.-F. Zhang, S.-L. Sun, Y.-H. Chen, L. Shu, L.-P. Yu, L. Zhu, L.-B. Song, Z. Cao, Effects of some nucleating agents on the supercooling of erythritol to be applied as phase change material, J. Therm. Anal. Calorim. (2017) 1–9. doi:10.1007/s10973-017-6296-2.
[86] P. Hu, P.-P. Zhao, Y. Jin, Z.-S. Chen, Experimental study on solid–solid phase change properties of pentaerythritol (PE)/nano-AlN composite for thermal storage, Sol. Energy. 102 (2014) 91–97. doi:10.1016/j.solener.2014.01.018.
[87] L. Dufour, Ueber das Gefrieren des Wassers und über die Bildung des Hagels, Ann. Phys. 190 (1862) 530–554. doi:10.1002/andp.18621901203.
[88] Rau, Walter, Eiskeimbildung durch dielektrische Polarisation, Z. Für Naturforschung. 6a (1951) 649–657.
[89] R.W. Salt, Effect of Electrostatic Field on Freezing of Supercooled Water and Insects, Science. 133 (1961) 458–459. doi:10.1126/science.133.3451.458.
[90] D.C. Blanchard, R.W. Salt, Electrostatic Field and Freezing, Science. 133 (1961) 1672–1672. doi:10.1126/science.133.3465.1672.
[91] M.H. Smith, R.F. Griffiths, J. Latham, The freezing of raindrops falling through strong electric fields, Q. J. R. Meteorol. Soc. 97 (1971) 495–505. doi:10.1002/qj.49709741409.
[92] G. Mandal, P. Pradeep Kumar, A laboratory study of ice nucleation due to electrical discharge, Atmospheric Res. 61 (2002) 115–123. doi:10.1016/S0169-8095(01)00129-6.
[93] H.R. Pruppacher, Electrofreezing of supercooled water, Pure Appl. Geophys. 104 (1973) 623–634. doi:10.1007/BF00875907.
[94] R.P. Hans, The effect of an external electric field on the supercooling of water drops, J. Geophys. Res. 68 (1963) 4463–4474. doi:10.1029/JZ068i015p04463.
[95] M. Roulleau, L.F. Evans, N. Fukuta, The Electrical Nucleation of Ice in Supercooled Clouds, J. Atmospheric Sci. 28 (1971) 737–740. doi:10.1175/1520-0469(1971)028<0737:TENOII>2.0.CO;2.
[96] M.A. Abbas, J. Latham, The Electrofreezing of Supercooled Water Drops, J. Meteorol. Soc. Jpn. Ser II. 47 (1969) 65–74. doi:10.2151/jmsj1965.47.2_65.
[97] R. Hickling, Nucleation of Freezing by Cavity Collapse and its Relation to Cavitation Damage, Nature. 206 (1965) 915–917. doi:10.1038/206915a0.
[98] I. Braslavsky, S.G. Lipson, Electrofreezing effect and nucleation of ice crystals in free growth experiments, Appl. Phys. Lett. 72 (1998) 264–266. doi:10.1063/1.120705.
[99] T. Shichiri, T. Nagata, Effect of electric currents on the nucleation of ice crystals in the melt, J. Cryst. Growth. 54 (1981) 207–210. doi:10.1016/0022-0248(81)90461-9.

[100] T. Shichiri, Y. Araki, Nucleation mechanism of ice crystals under electrical effect, J. Cryst. Growth. 78 (1986) 502–508. doi:10.1016/0022-0248(86)90152-1.
[101] T. Hozumi, A. Saito, S. Okawa, K. Watanabe, Effects of electrode materials on freezing of supercooled water in electric freeze control, Int. J. Refrig. 26 (2003) 537–542. doi:10.1016/S0140-7007(03)00008-2.
[102] H. Kumano, T. Hirata, K. Mitsuishi, K. Ueno, Experimental study on effect of electric field on hydrate nucleation in supercooled tetra-n-butyl ammonium bromide aqueous solution, Int. J. Refrig. 35 (2012) 1266–1274. doi:10.1016/j.ijrefrig.2012.03.005.
[103] T. Ohachi, M. Hamanaka, H. Konda, S. Hayashi, I. Taniguchi, T. Hashimoto, Y. Kotani, Electrical nucleation and growth of NaCH3COO·3H2O, J. Cryst. Growth. 99 (1990) 72–76. doi:10.1016/0022-0248(90)90486-5.
[104] Y. Yoshii, M. Kuraoka, K. Sengoku, T. Ohachi, Induction time and three-electrode current vs. voltage characteristics for electrical nucleation of concentrated solutions of sodium acetate trihydrate, J. Cryst. Growth. 237–239, Part 1 (2002) 414–418. doi:10.1016/S0022-0248(01)01823-1.
[105] T. Munakata, S. Nagata, Electrical Initiation of Solidification and Preservation of Supercooled State for Sodium Acetate Trihydrate, (2010) 383–388. doi:10.1115/IHTC14-22148.
[106] N.R. Jankowski, F.P. McCluskey, Electrical Supercooling Mitigation in Erythritol, (2010) 409–416. doi:10.1115/IHTC14-22306.
[107] S.W. Young, MECHANICAL STIMULUS TO CRYSTALLIZATION IN SUPER-COOLED LIQUIDS.1, J. Am. Chem. Soc. 33 (1911) 148–162. doi:10.1021/ja02215a003.
[108] S.W. Young, W.J.V. Sicklen, THE MECHANICAL STIMULUS TO CRYSTALLIZATION. 5, J. Am. Chem. Soc. 35 (1913) 1067–1078. doi:10.1021/ja02198a002.
[109] G.G. Goyer, T.C. Bhadra, S. Gitlin, Shock Induced Freezing of Supercooled Water, J. Appl. Meteorol. 4 (1965) 156–160. doi:10.1175/1520-0450(1965)004<0156:SIFOSW>2.0.CO;2.
[110] J.D. Hunt, K.A. Jackson, Nucleation of Solid in an Undercooled Liquid by Cavitation, J. Appl. Phys. 37 (1966) 254–257. doi:10.1063/1.1707821.
[111] B.E. Noltingk, E.A. Neppiras, Cavitation produced by Ultrasonics, Proc. Phys. Soc. Sect. B. 63 (1950) 674. doi:10.1088/0370-1301/63/9/305.
[112] M.A. Rogerson, S.S.S. Cardoso, Solidification in heat packs: I. Nucleation rate, AIChE J. 49 (2003) 505–515. doi:10.1002/aic.690490220.
[113] M.A. Rogerson, S.S.S. Cardoso, Solidification in heat packs: II. Role of cavitation, AIChE J. 49 (2003) 516–521. doi:10.1002/aic.690490221.
[114] J.D. Hunt, K.A. Jackson, Nucleation of the Solid Phase by Cavitation in an Undercooled Liquid which expands on Freezing, Nature. 211 (1966) 1080–1081. doi:10.1038/2111080b0.
[115] M.S. Plesset, The Dynamics of Cavitation Bubbles, J. Appl. Mech. 16 (1949) 277–282.
[116] W. Lauterborn, OPTIC CAVITATION, J. Phys. Colloq. 40 (1979) C8-273-C8-278. doi:10.1051/jphyscol:1979847.
[117] H. Frenzel, H. Schultes, Luminescenz im ultraschallbeschickten Wasser, Z. Für Phys. Chem. 27B (1934) 421–424. doi:10.1515/zpch-1934-2737.
[118] D.F. Gaitan, L.A. Crum, C.C. Church, R.A. Roy, Sonoluminescence and bubble dynamics for a single, stable, cavitation bubble, J. Acoust. Soc. Am. 91 (1992) 3166–3183. doi:10.1121/1.402855.
[119] M.P. Brenner, S. Hilgenfeldt, D. Lohse, Single-bubble sonoluminescence, Rev. Mod. Phys. 74 (2002) 425.
[120] T. Hozumi, A. Saito, S. Okawa, Effect of ultrasonic waves on freezing of supercooled water, Adv. Cold-Reg. Therm. Eng. Sci. (1999) 65–72.
[121] R. Chow, R. Mettin, B. Lindinger, T. Kurz, W. Lauterborn, The importance of acoustic cavitation in the sonocrystallisation of ice-high speed observations of a single acoustic bubble, in: IEEE Symp. Ultrason. 2003, 2003: pp. 1447-1450 Vol.2. doi:10.1109/ULTSYM.2003.1293177.
[122] K. Nakagawa, A. Hottot, S. Vessot, J. Andrieu, Influence of controlled nucleation by ultrasounds on ice morphology of frozen formulations for pharmaceutical proteins freeze-drying, Chem. Eng. Process. Process Intensif. 45 (2006) 783–791. doi:10.1016/j.cep.2006.03.007.

[123] T. Inada, X. Zhang, A. Yabe, Y. Kozawa, Active control of phase change from supercooled water to ice by ultrasonic vibration 1. Control of freezing temperature, Int. J. Heat Mass Transf. 44 (2001) 4523–4531. doi:10.1016/S0017-9310(01)00057-6.
[124] Y. Liu, Y. Liu, P. Hu, X. Li, R. Gao, Q. Peng, L. Wei, The effects of graphene oxide nanosheets and ultrasonic oscillation on the supercooling and nucleation behavior of nanofluids PCMs, Microfluid. Nanofluidics. 18 (2015) 81–89. doi:10.1007/s10404-014-1411-1.
[125] N. Lyczko, F. Espitalier, O. Louisnard, J. Schwartzentruber, Effect of ultrasound on the induction time and the metastable zone widths of potassium sulphate, Chem. Eng. J. 86 (2002) 233–241. doi:10.1016/S1385-8947(01)00164-4.
[126] K. Seo, S. Suzuki, T. Kinoshita, I. Hirasawa, Effect of Ultrasonic Irradiation on the Crystallization of Sodium Acetate Trihydrate Utilized as Heat Storage Material, Chem. Eng. Technol. 35 (2012) 1013–1016. doi:10.1002/ceat.201100680.
[127] E. Miyasaka, M. Takai, H. Hidaka, Y. Kakimoto, I. Hirasawa, Effect of ultrasonic irradiation on nucleation phenomena in a Na2HPO4 · 12H2O melt being used as a heat storage material, Ultrason. Sonochem. 13 (2006) 308–312. doi:10.1016/j.ultsonch.2005.05.006.
[128] F. Baillon, F. Espitalier, C. Cogné, R. Peczalski, O. Louisnard, 28 - Crystallization and freezing processes assisted by power ultrasound, in: Power Ultrason., Woodhead Publishing, Oxford, 2015: pp. 845–874. doi:10.1016/B978-1-78242-028-6.00028-4.
[129] S.L. Hem, The effect of ultrasonic vibrations on crystallization processes, Ultrasonics. 5 (1967) 202–207. doi:10.1016/0041-624X(67)90061-3.
[130] Z. Guo, A.G. Jones, N. Li, S. Germana, High-speed observation of the effects of ultrasound on liquid mixing and agglomerated crystal breakage processes, Powder Technol. 171 (2007) 146–153. doi:10.1016/j.powtec.2006.10.026.
[131] R. Chow, R. Blindt, R. Chivers, M. Povey, The sonocrystallisation of ice in sucrose solutions: primary and secondary nucleation, Ultrasonics. 41 (2003) 595–604. doi:10.1016/j.ultras.2003.08.001.
[132] R. Chow, R. Blindt, A. Kamp, P. Grocutt, R. Chivers, The microscopic visualisation of the sonocrystallisation of ice using a novel ultrasonic cold stage, Ultrason. Sonochem. 11 (2004) 245–250. doi:10.1016/j.ultsonch.2004.01.018.
[133] R. Chow, R. Blindt, R. Chivers, M. Povey, A study on the primary and secondary nucleation of ice by power ultrasound, Ultrasonics. 43 (2005) 227–230. doi:10.1016/j.ultras.2004.06.006.
[134] X. Zhang, T. Inada, A. Yabe, S. Lu, Y. Kozawa, Active control of phase change from supercooled water to ice by ultrasonic vibration 2. Generation of ice slurries and effect of bubble nuclei, Int. J. Heat Mass Transf. 44 (2001) 4533–4539. doi:10.1016/S0017-9310(01)00058-8.
[135] H. Harzali, F. Espitalier, O. Louisnard, A. Mgaidi, Sono-crystallization of ZnSO4 · 7H20, Phys. Procedia. 3 (2010) 965–970. doi:10.1016/j.phpro.2010.01.124.
[136] L. Wei, K. Ohsasa, Supercooling and Solidification Behavior of Phase Change Material, ISIJ Int. 50 (2010) 1265–1269. doi:10.2355/isijinternational.50.1265.
[137] G. Zeng, H. Li, S. Luo, X. Wang, J. Chen, Effects of ultrasonic radiation on induction period and nucleation kinetics of sodium sulfate, Korean J. Chem. Eng. 31 (2014) 807–811. doi:10.1007/s11814-013-0290-6.
[138] A. Hottot, K. Nakagawa, J. Andrieu, Effect of ultrasound-controlled nucleation on structural and morphological properties of freeze-dried mannitol solutions, Chem. Eng. Res. Des. 86 (2008) 193–200. doi:10.1016/j.cherd.2007.11.009.
[139] L. Qiu, L. Shi, Z. Liu, K. Xie, J. Wang, S. Zhang, Q. Song, L. Lu, Effect of power ultrasound on crystallization characteristics of magnesium ammonium phosphate, Ultrason. Sonochem. 36 (2017) 123–128. doi:10.1016/j.ultsonch.2016.11.019.
[140] E.P. Ona, S. Ozawa, Y. Kojima, H. Matsuda, H. Hidaka, H. Kakiuchi, M. Sato, Effect of Ultrasonic Irradiation Parameters on the Supercooling Relaxation Behavior of PCM, J. Chem. Eng. Jpn. 36 (2003) 799–805. doi:10.1252/jcej.36.799.
[141] A. Kordylla, S. Koch, F. Tumakaka, G. Schembecker, Towards an optimized crystallization with ultrasound: Effect of solvent properties and ultrasonic process parameters, J. Cryst. Growth. 310 (2008) 4177–4184. doi:10.1016/j.jcrysgro.2008.06.057.

[142] M. Saclier, R. Peczalski, J. Andrieu, Effect of ultrasonically induced nucleation on ice crystals' size and shape during freezing in vials, Chem. Eng. Sci. 65 (2010) 3064–3071. doi:10.1016/j.ces.2010.01.035.
[143] U.N. Hatkar, P.R. Gogate, Ultrasound Assisted Cooling Crystallization of Sodium Acetate, Ind. Eng. Chem. Res. 51 (2012) 12901–12909. doi:10.1021/ie202220q.
[144] A. Jabbari-Hichri, R. Peczalski, P. Laurent, Ultrasonically triggered freezing of aqueous solutions: Influence of initial oxygen content on ice crystals′ size distribution, J. Cryst. Growth. 402 (2014) 78–82. doi:10.1016/j.jcrysgro.2014.05.010.
[145] M.D. Luque de Castro, F. Priego-Capote, Ultrasound-assisted crystallization (sonocrystallization), Ultrason. Sonochem. 14 (2007) 717–724. doi:10.1016/j.ultsonch.2006.12.004.
[146] Montes Quiroz, William, Experimental study of the stability of an acoustic single bubble. Application to the ice nucleation induced by cavitation, Toulouse, 2014.
[147] T. Hozumi, A. Saito, S. Okawa, T. Matsui, Freezing phenomena of supercooled water under impacts of ultrasonic waves, Int. J. Refrig. 25 (2002) 948–953. doi:10.1016/S0140-7007(01)00104-9.
[148] H. Kimura, J. Kai, Phase change stability of sodium acetate trihydrate and its mixtures, Sol. Energy. 35 (1985) 527–534. doi:10.1016/0038-092X(85)90121-5.
[149] K. Ohsaka, E.H. Trinh, Dynamic nucleation of ice induced by a single stable cavitation bubble, Appl. Phys. Lett. 73 (1998) 129–131. doi:10.1063/1.121706.
[150] Y.J. Lü, W.J. Xie, B. Wei, Observation of ice nucleation in acoustically levitated water drops, Appl. Phys. Lett. 87 (2005) 184107. doi:10.1063/1.2126801.
[151] Y.J. Lü, B. Wei, Supercooling of aqueous NaCl and KCl solutions under acoustic levitation, J. Chem. Phys. 125 (2006) 144503. doi:10.1063/1.2358134.
[152] B. Krämer, O. Hübner, H. Vortisch, L. Wöste, T. Leisner, M. Schwell, E. Rühl, H. Baumgärtel, Homogeneous nucleation rates of supercooled water measured in single levitated microdroplets, J. Chem. Phys. 111 (1999) 6521–6527. doi:10.1063/1.479946.
[153] J.W. MULLIN, K.D. RAVEN, Nucleation in Agitated Solutions, Nature. 190 (1961) 251–251. doi:10.1038/190251a0.
[154] J.W. Mullin, K.D. Raven, Influence of Mechanical Agitation on the Nucleation of Some Aqueous Salt Solutions, Nature. 195 (1962) 35–38. doi:10.1038/195035a0.
[155] M. Kamalipour, S.A.M. Dehghani, A. Naseri, S. Abbasi, Role of agitation and temperature on calcium sulfate crystallization in water injection process, J. Pet. Sci. Eng. 151 (2017) 362–372. doi:10.1016/j.petrol.2016.12.039.
[156] L. Desgrosseilliers, M.A. White, D. Groulx, Thermal energy storage apparatus, US20180017337A1, 2018. https://patents.google.com/patent/US20180017337A1/en (accessed August 29, 2018).
[157] Latentwärmespeicher mit einer Vorrichtung zur Auslösung der Kristallisation, EP3056848B1, 2018. https://patents.google.com/patent/EP3056848B1/en?assignee=hm+heizkorper&oq=hm+heizkorper (accessed August 29, 2018).
[158] M. Dannemand, S. Furbo, SUPERCOOLING STABILITY OF SODIUM ACETATE TRIHYDRATE COMPOSITES IN MULTIPLE HEAT STORAGE, (2018) 5.
[159] A.J. Bissell, D. Oliver, C.R. Pulham, Improved Phase Change Compositions, 2016.
[160] H. Huntemann, M. Baumann, I. Parchmann, H. Schmidkunz, Effiziente Energienutzung mit Latentwärmespeichern. Ein interessantes Thema für den Chemieunterricht, CHEMKON. 9 (2002) 77–85. doi:10.1002/1521-3730(200205)9:2<77::AID-CKON77>3.0.CO;2-1.
[161] L.L. Vasiliev, V.S. Burak, A.G. Kulakov, D.A. Mishkinis, P.V. Bohan, Latent heat storage modules for preheating internal combustion engines: application to a bus petrol engine, Appl. Therm. Eng. 20 (2000) 913–923. doi:10.1016/S1359-4311(99)00061-7.